Washington University in St. Louis
Washington University Open Scholarship

McKelvey School of Engineering Theses & Dissertations

McKelvey School of Engineering

Summer 8-2015

System Level and Reactor Level Simulations of Chemical Looping Combustion and Chemical Looping with Oxygen Uncoupling

Xiao Zhang
Washington University in St Louis

Follow this and additional works at: https://openscholarship.wustl.edu/eng_etds

 Part of the Engineering Commons

Recommended Citation

Zhang, Xiao, "System Level and Reactor Level Simulations of Chemical Looping Combustion and Chemical Looping with Oxygen Uncoupling" (2015). *McKelvey School of Engineering Theses & Dissertations*. 113.
https://openscholarship.wustl.edu/eng_etds/113

This Thesis is brought to you for free and open access by the McKelvey School of Engineering at Washington University Open Scholarship. It has been accepted for inclusion in McKelvey School of Engineering Theses & Dissertations by an authorized administrator of Washington University Open Scholarship. For more information, please contact digital@wumail.wustl.edu.

WASHINGTON UNIVERSITY IN ST. LOUIS

School of Engineering and Applied Science

Department of Mechanical Engineering and Materials Science

Thesis Examination Committee:
Ramesh Agarwal, Chair
David Peters
Kenneth Jerina

System Level and Reactor Level Simulations of Chemical Looping Combustion and Chemical Looping with Oxygen Uncoupling

by

Xiao Zhang

A thesis presented to the School of Engineering
of Washington University in St. Louis in partial fulfillment of the
requirements for the degree of
Master of Science

August 2015

Saint Louis, Missouri

Contents

List of Figures

List of Tables

Acknowledgments

I would like to express my sincere gratitude to my academic advisor Dr. Ramesh K. Agarwal for his patient guidance, inspiring encouragement and continuous support. Without his help, my thesis has no chance to be accomplished. It is my great honor to be under his direction.

I also want to thank all of my colleagues working in the Computational Fluid Dynamics Laboratory of the Department of Mechanical Engineering & Materials Science at Washington University in St. Louis, for creating a wonderful learning environment. Special thanks go to Subhodeep Banerjee for providing technical advice and sharing his wide breath of knowledge.

I especially want to thank my family for caring and supporting me. They are always there for me no matter what.

Xiao Zhang

Washington University in St. Louis
August 2015

ABSTRACT OF THE THESIS

System Level and Reactor Level Simulation of Chemical Looping Combustion and Chemical Lopping with Oxygen Uncoupling

by

Xiao Zhang

Master of Science in Mechanical Engineering

Washington University in St. Louis, 2015

Research Advisor: Professor Ramesh Agarwal

Chemical-looping combustion (CLC) and chemical-looping with oxygen uncoupling (CLOU) are currently considered as the leading technology alternatives for reducing the economic cost of CO2 capture. In this thesis, CLC and CLOU models are established in ASPEN Plus and are validated against the experimental work of Sahir el al. [1] and Abad et al. [2] respectively. The energy balance of each major component in flow sheet model of both CLC and CLOU process in ASPEN Plus, e.g. the fuel and air reactors and air/flue gas heat exchangers is examined. In order to investigate the effect of air flow rate and oxygen carrier on the overall energy output, several case studies for different types of coal are conducted for the CLC and CLOU process models, and the optimal ratio of coal feeding rate, air flow rate and oxygen carrier rate is obtained for maximum energy output for three types of coal and four types of oxygen carriers. Scaled-up cases are also conducted to investigate the influence of increase in the coal, air flow and oxygen carriers feeding rates. In addition, reactor level simulations are performed to investigate the physics of fluidized beds in a complete CLC apparatus used by NETL by coupling the CFD hydrodynamic solver FLUENT with

a discrete element method (DEM) describing the movement of coal particles in the air and fuel reactors, loop seal, cyclone and down-comer. Velocity and pressure fields for cold flow are obtained. Circulation of the coal particles occurs due to adequate pressure difference in the entire CLC system and the injection velocity of air.

Chapter 1 Introduction

1.1 Motivation

Climate change due to global warming has drawn a great deal of attention in recent years among people all over the world; it is already causing a cascade of negative effects on the environment, human society, and nature. The bulk of humanity's energy needs are currently met through the combustion of fossil fuels like coal, oil, and natural gas. About 60% of global electricity generation relies upon fossil fuels to generate the heat needed to power steam-driven turbines. Burning these fuels results in the production of carbon dioxide (CO_2) – the primary heat-trapping, greenhouse gas responsible for global warming.

"While the Kyoto Protocol, which aims to reduce greenhouse gas emissions, is slowly impacting on energy markets, scientists are increasingly advising policymakers that carbon emission reductions beyond 60% are needed over the next 40-50 years." Although renewable energy from sources such as wind, solar, biomass, hydro, wave and tidal offers a safe transition to a low carbon economy, combustion of fossil fuels will remain a major source of energy for several decades in the future.

Chemical-looping combustion (CLC) and chemical-looping with oxygen uncoupling (CLOU) are regarded as two novel fossil fuel combustion technologies, which require less energy for CO_2 capture compared to other technologies such as absorption/adsorption and oxy-fuel. A large number of experiments and simulations for laboratory and pilot scale plants based on CLC and CLOU technology have been conducted in last decade. The goal of this thesis is to conduct process and reactor level simulations of both CLC and CLOU process.

1.2 Brief Review of Literature

Sahir et al. [1] were among the first to employ the ASPEN Plus software to model the CLC process using an iron-based oxygen carrier and a copper-based oxygen carrier, using a Wyoming Powder

River Basin coal. They successfully evaluated the material and energy requirements for a pilot-scale unit by incorporating insights from previously reported CLC kinetics studies from lab-scale units.

Abad et al. [2] were the first to demonstrate the proof of concept of the CLOU technology by burning coal in a 1.5 kW_{th} continuously operated unit consisting of two interconnected fluidized-bed reactors. A bituminous coal was used as fuel. An oxygen-carrier prepared by spray drying containing 60 wt.% CuO and $MgAl_2O_4$ as supporting material was used as oxygen-carrier. The effects of fuel-reactor temperature, coal feeding rate, and solids circulation flow rate on the combustion and on the CO_2 capture efficiencies were investigated. Results obtained were analyzed and discussed in order to be useful for scale-up of a CLOU process fuelled by coal. The above two papers have been used in this thesis for creating a model of CLC and CLOU process in ASPEN Plus at system level.

At reactor level, Parker [3] has created a full three-dimensional CFD model of an entire chemical looping combustion (CLC) system using coal as fuel source. The whole system consists of an oxidation reactor, fuel reactor, riser and cyclone. The particle-fluid dynamics in the CLC loop is modeled using the CPFD numerical method which is implemented in Barracuda software package from CPFD Software, LLC. Multiple heterogeneous reactions are considered in the CLC model including the oxidation and reduction of methane, carbon monoxide and hydrogen reacted with the ilmenite carrier, steam gasification, carbon dioxide gasification, and the water gas shift reactions. Also within each coal particle, the temperature-dependent devolatilization and moisture release is included. In this thesis, the CFD simulation of the NETL-CLC apparatus, considered by Parker [3], is conducted using CFD-DEM approach employing the ANSYS Fluent software.

1.3 Scope of the Thesis

The thesis addresses two problems in novel combustion technologies, which are chemical looping combustion (CLC) and chemical looping with oxygen uncoupling (CLOU). For CLC process, system level simulation is conducted in ASPEN Plus and reactor level simulation is achieved using ANSYS Fluent. The geometry and mesh is also created using Design Modeler and mesh tool in ANSYS software package. For CLOU process, system level simulation is also conducted in ASPEN

Plus. Maximum energy output and optimal ratio between coal, air flow rate and oxygen carrier feeding rate are the major concerns for both of the CLC and CLOU process level simulation. As for reactor level simulation of CLC, particle recirculation of cold flow is examined using coupled CFD/DEM approach.

Chapter 2 Chemical-Looping Combustion (CLC)

2.1 Introduction

Coal-fired power plants contribute to significant CO_2 emissions; this reality has driven research in recent years on investigation of combustion processes that can capture CO_2 with reduced energy penalty. One technology that is showing great promise for high-efficiency low-cost carbon capture is the Chemical-Looping Combustion (CLC) process. In contrast to other methods for CO_2 separation from flue gas such as oxy-combustion, chemical absorption, and physical adsorption, the CLC is an advanced technology that creates and captures an almost pure and concentrated CO_2 stream with relatively less energy requirement [4,5]. Several theoretical and experimental studies have demonstrated the potential of CLC to capture almost pure CO_2 very efficiently [6-9]. CLC employs a dual fluidized bed system with circulating fluidized bed process where an oxygen carrier (OC) is used as a bed material providing the oxygen for combustion in the fuel reactor. The reduced OC is then transferred to a second bed and re-oxidized by the atmospheric air [10-12] in an air reactor before it is returned to the fuel reactor to complete the loop. Figure 2.1 shows the loop of CLC process. Because of the absence of air in the fuel reactor, the combustion products are not diluted by other gases (e.g., N_2), resulting in high purity CO_2 available at the outlet of the fuel reactor. Thus, the CLC process for power generation provides a sequestration-ready CO_2 stream directly after combustion, without the need for using costly gas separation techniques to purify CO_2 from the flue stream. CLC therefore holds significant promise as a next generation combustion technology due to its potential for pre-capturing almost pure CO_2 emission with very limited effect on the efficiency of the power plant.

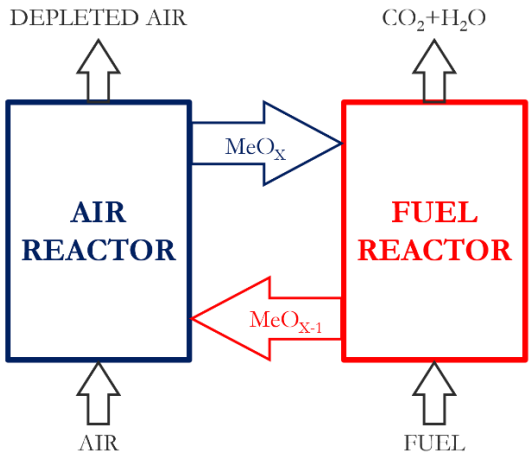

Figure 2.1 Sketch the of CLC process

In this section, system level simulation of CLC process is described using the ASPEN Plus software. ASPEN Plus is a process simulation software that simulates chemical processes at system level using basic engineering relationships such as mass and energy balance, and multi-phase and chemical reaction models. It consists of flow sheet simulations to calculate stream properties such as flow rate and mass composition given various chemical processes and operating conditions. In this section, first a model of the CLC process is developed and validated against the experimental data; it is then applied to conduct parametric studies for optimal energy output. These studies provide valuable insight into the design and operating conditions required in an industrial-scale CLC plant to optimize the energy output with almost pure CO_2 capture with little energy penalty.

2.2 System Level Simulation of the CLC Process

The CLC process simulation model in ASPEN Plus is developed and validated following the experimental work of Sahir et al [1]. The physical and chemical properties of the Colombian coal used as the solid fuel in the experiment are summarized in Table 2.1.

Table 2.1 Physical and chemical properties of Colombian coal

Proximate Analysis (wt. %)				Ultimate Analysis (wt. %)					Energy
Moisture	Volatile matter	Fixed carbon	Ash	C	H	N	S	O	LHV (MJ/kg)
3.3	37.0	54.5	5.2	80.7	5.5	1.7	0.6	11.5	29.1

The schematic of the flow sheet for this simulation is shown in Figure 2.2. The coal is first pulverized and dried before it is pressurized and introduced into a shell gasifier to be partially oxidized to form syngas. The molar ratio of steam and carbon is maintained at unity for the process model. The syngas composition at the gasifier outlet is 34.5% CO, 50.3% H_2, 12.3% H_2O, and 2.4% CO_2. The syngas is converted completely to CO_2 and H_2O in the fuel reactor while the Fe_2O_3 in the oxygen carrier is reduced to Fe_3O_4. The oxygen carrier material used is a mixture of 60 wt. % Fe_2O_3 and 40 wt. % inert Al_2O_3 as support. The outflow from the fuel reactor is a concentrated stream of H_2O and CO_2. After condensing the stream, high purity CO_2 is obtained. The reduced oxygen carrier is fed into the air reactor where the oxidation reaction takes place with an 80% conversion of Fe_3O_4 to Fe_2O_3.

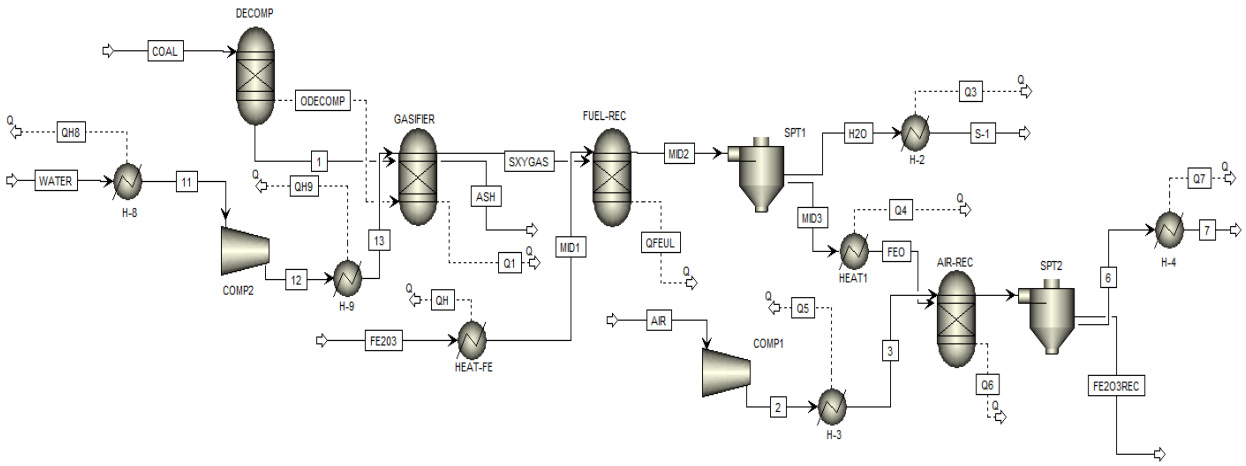

Figure 2.2 Flow sheet of the CLC model in ASPEN Plus

The various process models used in the ASPEN Plus shown in flow sheet in Figure 2.2 are summarized in Table 2.2. The coal devolatilization is defined by the RYIELD reactor, followed by

the gasification of coal represented by the RGIBBS reactor. Another RGIBBS reactor defines the actual syngas combustion and the corresponding reduction of the oxygen carrier. These blocks together represent the fuel reactor. The flow sheet within the ASPEN Plus simulation package cannot model this entire reaction with one reactor. As a result, the fuel reactor simulation is broken down into several different reactor simulations. The air reactor is also modeled as an RGIBBS reactor.

Table 2.2 Process models used in different parts of the CLC process in ASPEN Plus

Name	Model	Function	Reaction formula
DECOMP	RYIELD	Coal devolatilization	Coal → volatile matter + char
BURN	RGIBBS	Gasification	Char + volatile matter → CO_2 + H_2O
FUEL-R	RSTOIC	Carrier reduction reaction	$3Fe_2O_3$ + CO/H_2 → $2Fe_3O_4$ + CO_2/H_2O
AIR-R	RSTOIC	Carrier oxidation reaction	$4Fe_3O_4$ + O_2 → $6Fe_2O_3$

For the purpose of validation, the energy balance of the CLC process model was analyzed using the input values from the work of Sahir et al [1]. The input values and the energy requirements for the various units and streams in Figure 2.2 are presented in Table 2.3; this will be referred to as the baseline case in rest of the paper. Energy is consumed mainly in the compressor processes. Compressed air is required in the air reactor to regenerate Fe_2O_3 from Fe_3O_4. The air compressor for the combustor compresses air to 18 atm. Another compressor is used to compress the steam for the gasifier. There is a large amount of energy produced in the air reactor, but the fuel reactor needs to be supplied with energy. This is because the net heat work in the fuel reactor is the summation of the heat work from the DECOMP, GASIFER, and FUEL-R blocks. Although FUEL-R produces energy because of the combustion of syngas, the combined energy requirement of DECOMP and GASIFIER are more than the energy produced in FUEL-R. Summing the energy requirements of each individual stream, the total energy obtained from the CLC process is 554.2 kW.

Table 2.3 Input values and energy balance for baseline case corresponding to the experiment of Sahir et al. [1]

Input values	Coal (kg/h)	100
	Steam (kg/h)	140
	Air Flow Rate (kg/h)	713
	Temperature of Fuel Reactor (ºC)	950
	Temperature of Air Reactor (ºC)	935
	Fe_2O_3 flow in the Fuel Reactor (kg/h)	5921
	Al_2O_3 in the System (kg/h)	3951
	Particle Density (kg/m³)	3200
Energy Balance (kW)	Fuel reactor	-161.8
	Air reactor	688.0
	Cool air reactor exhaust	135.4
	Cool flue gas	148.3
	Cool OC for air reactor	40.9
	Reheat OC for fuel reactor	-42.7
	Heat steam	-69.8
	Heat air	-184.1
	Net	554.2

The results shown in Table 2.3 for the baseline case with a coal feed rate of 100 kg/h are in excellent agreement with those reported by Sahir et al [1]. These calculations validate our CLC model developed in ASPEN Plus.

2.3 Investigation of the Effect of Various Parameters on the Energy Output of the CLC Process Simulation

With the successful validation of the process simulation of the CLC model in the previous section, the ASPEN Plus simulation is expanded to consider the effect of varying the air flow rate and the oxygen carrier feeding rate. Additional scaled-up simulations are also conducted to determine these effects on an industrial scale power plant.

2.3.1 Effect of Varying the Air Flow Rate on Energy Output of Baseline Case with 100 kg/h Coal Feeding Rate

The recent paper of Mukherjee et al. [13] suggests that it is favorable to operate the air reactor of the CLC process at higher temperatures with excess air supply in order to achieve higher power efficiency. In order to evaluate the effect of air supply on energy output, we consider the baseline case of Table 2.3 and vary the air flow rate. The results are presented in Figure 2.3 and Table A.1. From Figure 2.3, it can be seen that with an increase in the air flow rate, the net energy output increases and achieves a maximum for a certain air flow rate. If the air flow rate is further increased from its maximum value (i.e., value corresponding to maximum energy output), the energy output starts decreasing albeit very slowly. This result implies that there exists a certain rate of air supply around 900 kg/h to obtain the maximum energy output for 100 kg/h of coal supply. At this flow rate in the air reactor, 131.06 kW of additional energy is generated, which is 23.6% more than the baseline case given in Table 2.3 indicating that the reaction in the air reactor is not complete for the baseline case. Excess air supply ensures the 80% conversion of Fe_3O_4 to Fe_2O_3.

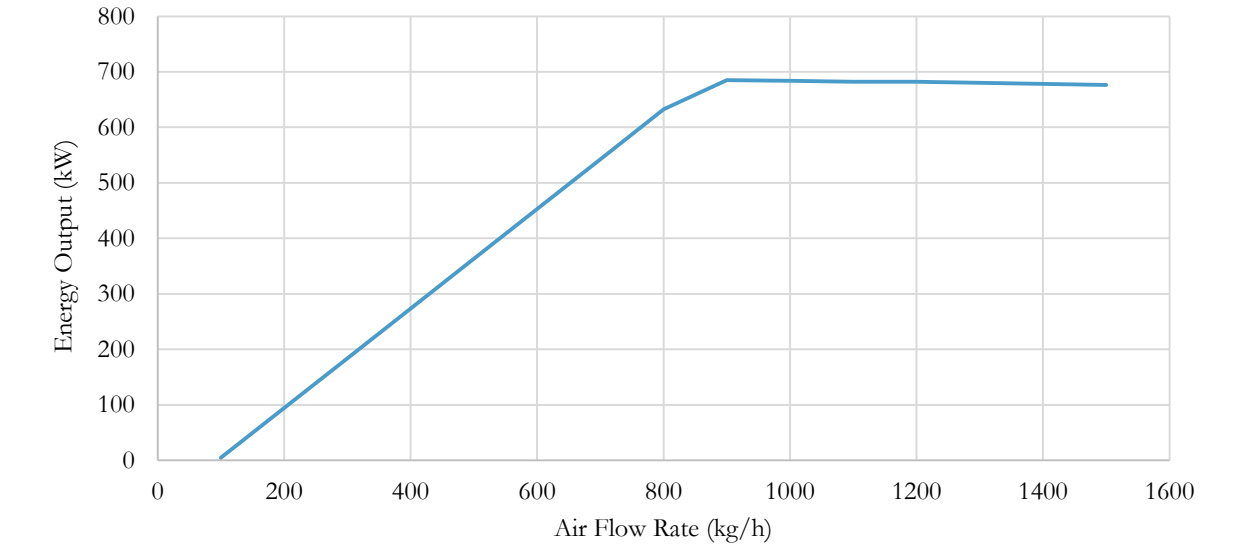

Figure 2.3 Energy output for various air flow rates for 100 kg/h of coal supply

2.3.2 Effect of Varying the Oxygen Carrier Feeding Rate on Energy Output of Baseline Case with 100 kg/h Coal Feed Rate

The oxygen carrier (OC) plays a vital role in the CLC process; it reacts with the syngas in the fuel reactor and reacts with the air in the air reactor. Both of these reactions contribute a large amount to the net energy output. Figure 2.4 and Table A.1–A.6 present the energy output for different OC feeding rates in the system with varying air flow rates. As expected, Figure 2.4 shows that for a given air flow rate, a higher OC feeding rate yields more energy output. However, when the OC feeding rate increases above a certain threshold value, the marginal increase in energy output by increasing the OC rate becomes extremely small. The red line in Figure 2.3 represents the baseline case (Fe_2O_3 at 5921 kg/h), for which the maximum energy output is 685.26 kW with 900 kg/h air flow rate. For the threshold Fe_2O_3 rate of 7000 kg/h, the maximum energy output of 824.33 kW occurs at the 1000 kg/h air flow rate. 138.97 kW of additional energy output is obtained by increasing the OC rate from 5921 kg/h to 7000 kg/h. Therefore, for maximum energy output with a coal feeding rate of 100 kg/h, the optimum rates of air flow and OC feeding are 1000 kg/h and 7000 kg/h respectively. In other words, the optimum ratio of Coal: Air: OC is 1: 10: 70.

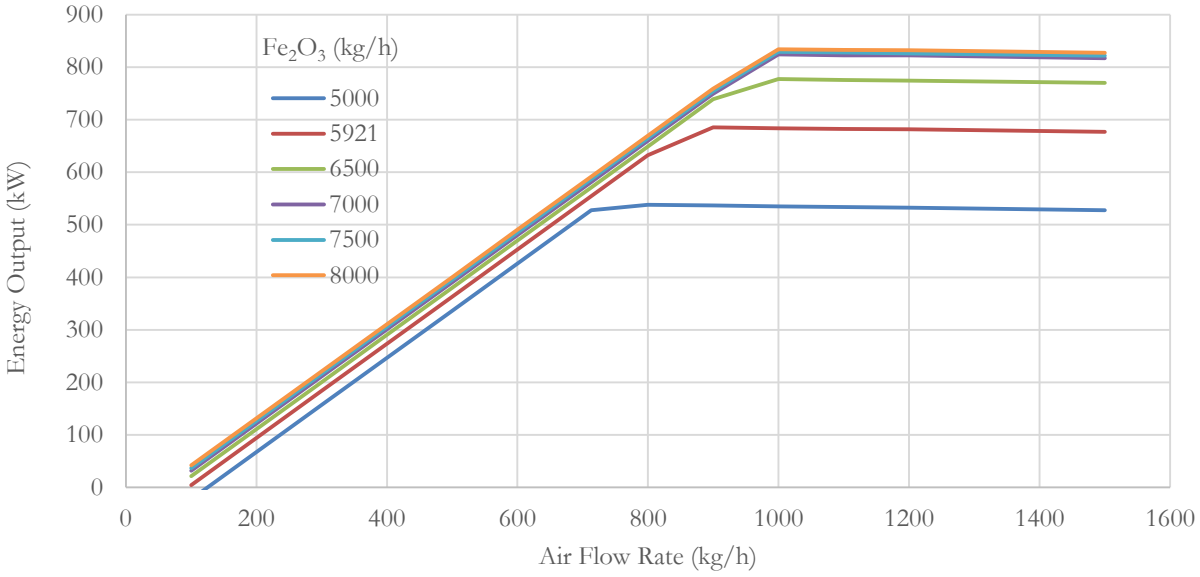

Figure 2.4 Energy output for various oxygen carrier feeding rates and air flow rates for 100 kg/h of coal supply

2.3.3 Scaled-up Simulation

Scaling up is an essential step for the realization and optimization of industrial-scale power plants. Two different scaled-up simulations were conducted to investigate the relationship between the coal feeding rate and energy output. The first scaled-up simulation employed the initial values of the baseline case and the other was based on the optimum values of coal: air supply: oxygen carrier rate. The details of the scaled-up simulations are given in Table A.7 and Table A.8 respectively. In both cases, the coal feeding rate is scaled up by a factor of up to 12. The OC feeding rate and air supply rate are also scaled-up accordingly to meet the demand of the increased coal feeding. Other modeling parameters such as the reactor efficiency and coal decomposition rate are considered unchanged for both the scaled up simulations. The total thermal power output for the scaled-up simulations is summarized in Figure 2.5 and Table 2.4 below. From Figure 2.5, it can be seen that the total power output increases linearly with increase in coal feeding rate. Considering the principles of energy and mass balance on which the ASPEN Plus modeling is based, linearity in the scaled-up results is expected since the non-linear effects (e.g., the energy loss at multiple locations in the flow sheet) are omitted in the modeling process.

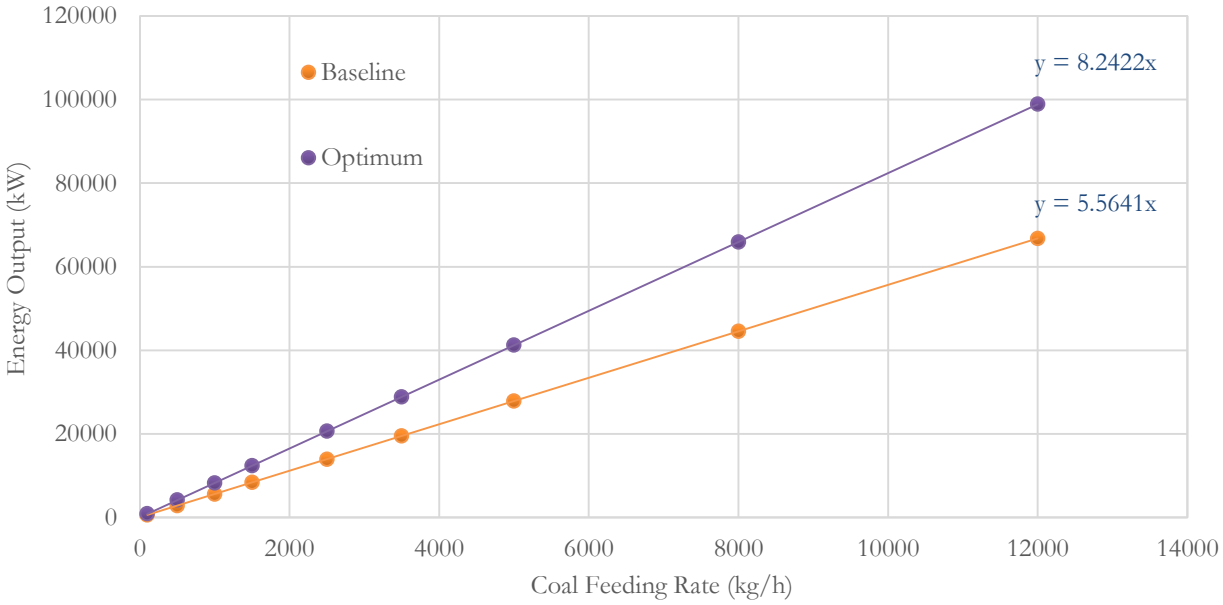

Figure 2.5 Energy output of two scaled-up simulations for various coal feeding rates

Table 2.4 Results of two scaled-up simulations for different ratios of Coal: Air: OC

Coal (kg/h)		100	500	1000	1500	2500	3500	5000	8000	12000
Energy output (kW)	Baseline	554.2	2782	5564	8346	13910	19474	27820	44513	66769
	Optimum	824.2	4121	8242	12363	20606	28847	41211	65936	98907

Based on these scaled-up simulations, the energy output for the baseline case is given by the equation

$$\text{Energy output} = 5.5641 \times \text{Coal feeding rate} \tag{2.1}$$

and the energy output for the optimum case is given by the equation

$$\text{Energy output} = 8.2422 \times \text{Coal feeding rate} \tag{2.2}$$

2.3.4 Validation of Optimum Values of Air Flow Rate and Oxygen Carrier Feeding Rate for Scaled-up Simulation

To demonstrate that the optimum values of air flow rate and OC feeding rate for maximum energy output are valid for the scaled-up simulations, three more cases with 12,000 kg/h coal feeding rate and varying rates of air flow and OC were studied, which are presented in Figure 2.6 and Tables A.9–A.11. Figure 2.6 shows that the maximum energy output occurs at 120,000 kg/h of air flow rate, and 840,000 kg/h of Fe_2O_3 feeding rate. This suggests that the optimum ratio of Coal: Air: OC in the system still holds for the scaled-up simulations; it is given by

$$\text{Coal feeding rate: Air flow rate: OC feeding rate} = 1: 10: 70 \tag{2.3}$$

Equation (2.3) is an important relationship among these three input parameters for obtaining the maximum energy output from a CLC-based power plant. This relationship can be used for the initial estimates in designing a CLC-based industrial-scale power plant.

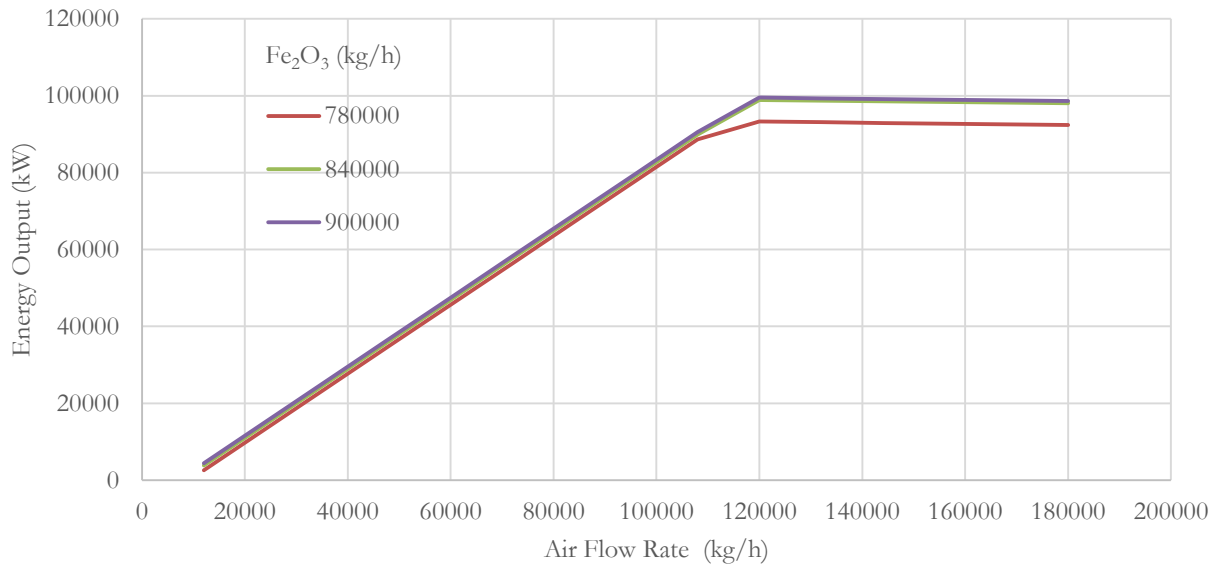

Figure 2.6 Energy output for different airflow rates and OC rates for a 12000 kg/h coal feeding rate

2.4 Energy Output of Different Types of Coals

All the results above are dependent on certain type of coal, the Colombian coal for which the physical and chemical properties are listed in Table 2.1. Now it is interesting to investigate the performance of different types of coal. Four types of coals are used in this thesis which are Colombian, Bituminous, Anthracite and Lignite. The proximate analysis and ultimate analysis of these coals are summarized in Table 2.5.

Table 2.5 Physical and chemical properties of four types coals

	Proximate Analysis (wt. %)				Ultimate Analysis (wt. %)					Energy
Coal name	Moisture	Volatile matter	Fixed carbon	Ash	C	H	N	S	O	LHV (MJ/kg)
Colombian	3.3	37.0	54.5	5.2	80.7	5.5	1.7	0.6	11.5	29.100
Bituminous	2.3	33.0	55.9	8.8	65.8	3.3	1.6	0.6	17.6	21.899
Anthracite	1.0	7.5	59.9	31.6	60.7	2.1	0.9	1.3	2.4	21.900
Lignite	12.6	28.6	33.6	25.2	45.4	2.5	0.6	5.2	8.5	16.250

2.4.1 Effect of Varying the Air Flow Rate on Energy Output of Four Types of Coals with 100 kg/h Coal Feeding Rate

Again in order to evaluate the effect of air supply on energy output, we conduct the same process modeling as described in section 2.3.1 by varying the air flow rate with coal feeding rate of 100 kg/h for four different types of coals. The results are presented in Figure 2.7 and Table A.1 for Colombian coal and in Tables A.12–A.14 for Bituminous, Anthracite and Lignite coal respectively. From Figure 2.7, it can be seen that with an increase in air flow rate, all four types of coal show the same trend that the net energy output increases and achieves a maximum for a certain air flow rate. Every coal type has a different inflection point which corresponds to the maximum energy output on the y-axis for a certain air flow rate shown on the x-axis. It can be seen that the inflection point is different depending upon the type of coal which is expected because of different properties of the coals as given in Table 2.5. By qualitative analysis, one can infer that higher the concentration of fixed carbon in a coal gives more fuel to burn, and the higher concentration of volatile matter and ash cost less energy to decompose the coal. Next, we determine the optimal ratio of Coal: Air: OC for the other three types of coal.

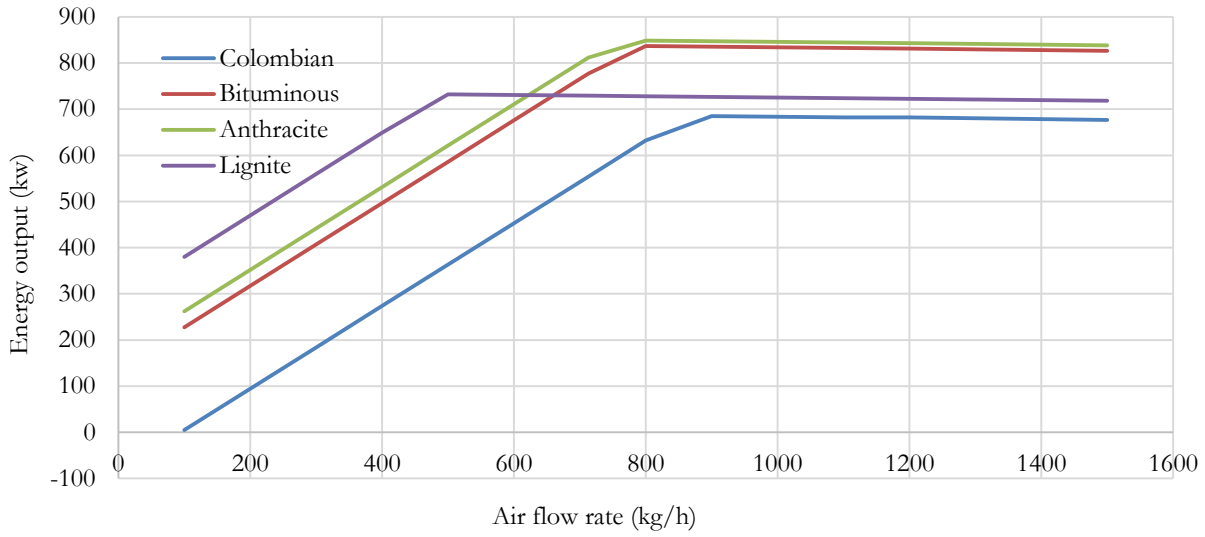

Figure 2.7 Energy output for various air flow rates for 100 kg/h of four types of coals supply

2.4.2 Effect of Varying the Oxygen Carrier Feeding Rate on Energy Output of Four Types of Coals with 100 kg/h Coal Feeding Rate

The effect of varying the oxygen carrier feeding rate on energy output of Colombian coal was shown in Figure 2.4 and Tables A.1–A.6. The results of other three types of coal–Bituminous, Anthracite and Lignite are presented in Figures 2.8–2.10 and Tables A.12–A.24. As expected, as with the Colombian coal, there is the maximum energy output based on optimal coal feeding rate: air flow rate: OC feeding rate for Bituminous, Anthracite and Lignite coal as well. Table 2.6 summarizes the maximum energy output and optimal ratio of Coal: Air: OC for four types of coal with 100 kg/h coal feed rate.

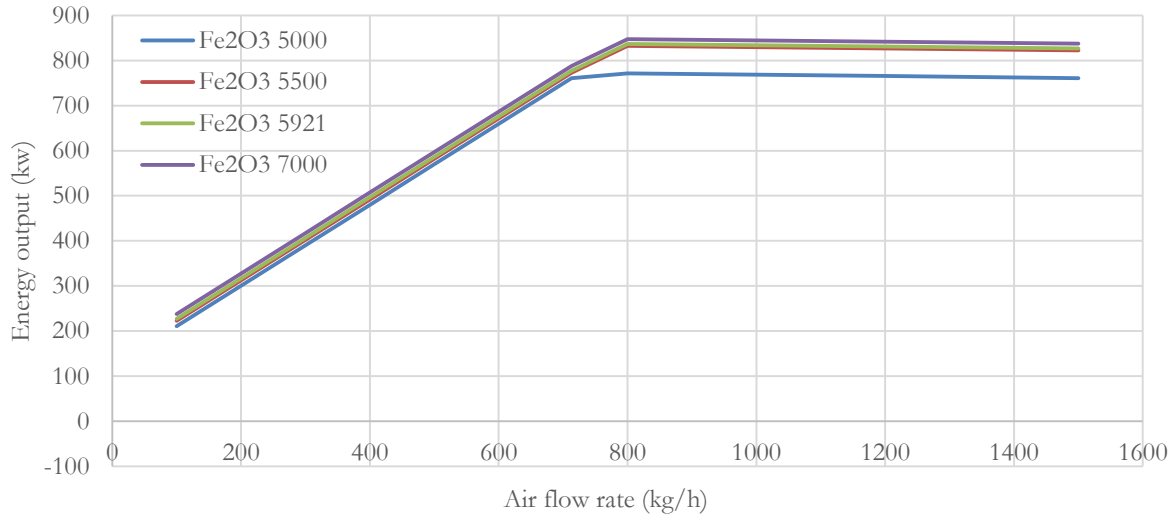

Figure 2.8 Energy output for various oxygen carrier feeding rates and air flow rates for 100 kg/h of Bituminous coal supply

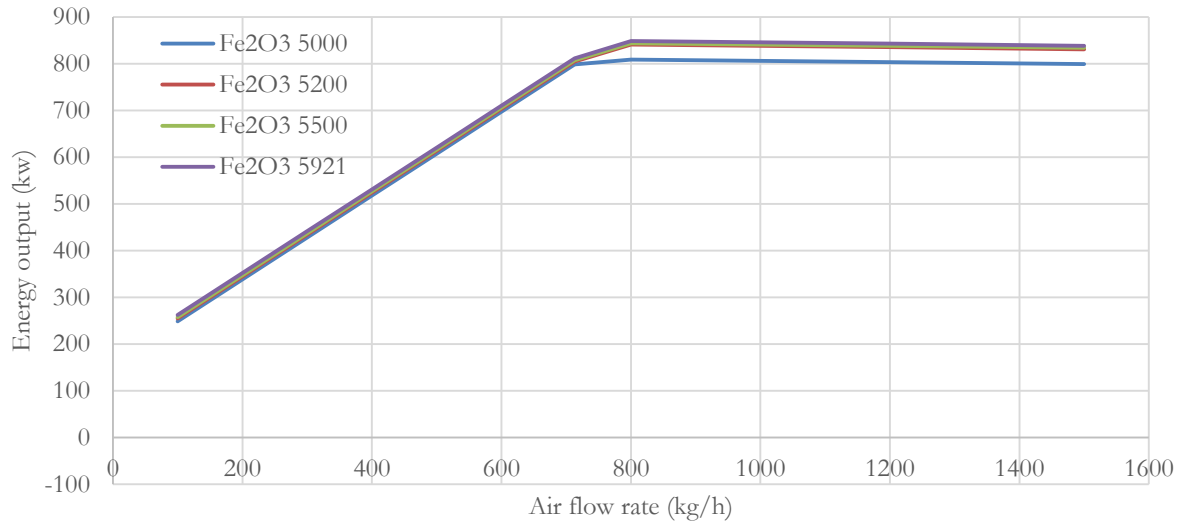

Figure 2.9 Energy output for various oxygen carrier feeding rates and air flow rates for 100 kg/h of Anthracites coal supply

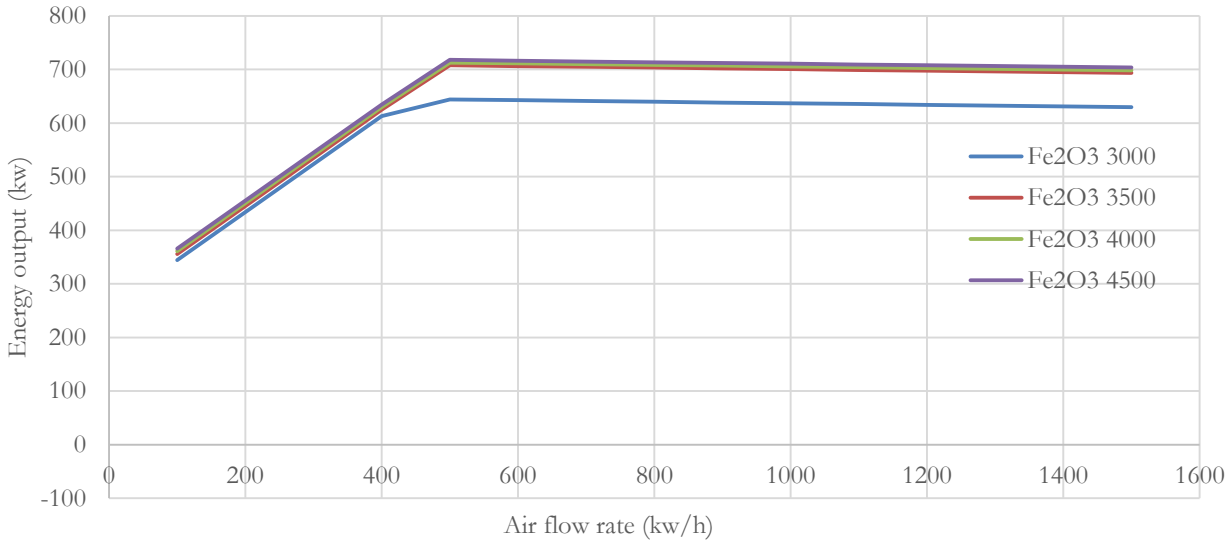

Figure 2.10 Energy output for various oxygen carrier feeding rates and air flow rates for 100 kg/h of Lignite coal supply

Table 2.6 Maximum energy output and optimal ratio of Coal: Air: OC for four types of coal with 100 kg/h coal feed rate

Coal Name	Maximum Energy (kw)	Optimal Ratio of Coal: Air: OC
Colombian	824.229	1: 70: 10
Bituminous	832.373	1: 55: 8
Anthracite	841.258	1: 52: 8
Lignite	707.905	1: 35: 5

2.5 Conclusion

In this chapter, ASPEN Plus is employed to model and study the complete CLC process from the coal gasification to the reduction and eventual re-oxidation of the oxygen carrier (OC). The CLC process model is validated following the work of Sahir et al [1]; it shows good agreement between the experimental data and the simulation results. Based on further studies on the effect of varying air flow rates and OC feeding rates, it is found that the maximization of energy output from CLC can be accomplished by using the optimum ratio of Coal: Air: OC in the system equal to 1: 10: 70 for Colombian coal. Compared to the baseline case based on the work of Sahir et al [1], a net increase in power of 48% can be obtained by increasing the air flow rate by 40.25% and the OC feeding rate by 18.22% to attain this optimum ratio for the Colombian coal for the given coal feeding rate of 100kg/h. Scaled-up simulations are also conducted using different coal feeding rates. The results show that the total power output is linear with increase in coal feeding rate. In general, such linearity is not expected for actual industrial-level scale-up since the ASPEN Plus system modeling software neglects miscellaneous energy losses in the system due to changes in the hydrodynamic characteristics of the two fluidized bed reactors. To account for the changes in the hydrodynamics characteristics, detailed hydrodynamic simulations are needed using the computational fluid dynamics software. Three other types of coal (Bituminous, Anthracite, and Lignite) are also investigated, and the optimal ratio of coal: airflow: OC is determined for each of these coal types. There are other parameters that may also influence the energy output such as the temperature and pressure.

Chapter 3 Chemical-Looping with Oxygen Uncoupling (CLOU)

3.1 Introduction

When solid fuel (e.g. coal) is utilized in a CLC system, it is often the case that the reactivity of char is low; it is due to the limited contact of oxygen carrier and gasified coal. An alternative process known as the chemical-looping with oxygen uncoupling (CLOU) has recently been proposed to overcome the low reactivity of the char gasification stage in the direct coal chemical-looping combustion. The CLOU process is based on a special material as oxygen carrier (OC) which can release gaseous oxygen at suitable temperatures in the fuel-reactor. In the fuel-reactor of CLOU, the fuel conversion is processed by different reactions. Since the fuel-reactor is a high-temperature and oxygen-deficient environment, the oxidized OC first decomposes to reduced OC and gaseous O_2:

$$2MeO_x \rightleftarrows 2MeO_{x-1} + O_2\,(g) \tag{3.1}$$

And the coal fed into the fuel reactor undergoes a two stage process. It first devolatilizes, producing a solid residue char and volatile matter as gas product:

$$\text{Coal} \rightarrow \text{char} + \text{volatiles (g)} + H_2O\,(g) \tag{3.2}$$

Then these combustibles are burnt immediately as in a normal combustion. The reduced OC is then transported to the air-reactor to be regenerated by absorbing oxygen from air, and becoming ready for a new cycle. It is worth noting that in the CLOU system coal does not have to be gasified first in the fuel-reactor since the oxygen release of OC and the combustion of char are usually far faster than the gasification of char. Thereby, a higher overall reaction rate in the fuel-reactor is attained, leading to much less OC inventory and lower circulation rate, and much higher carbon conversion, CO_2 capture efficiency and combustion efficiency.

In a previous study, Zhou et al. [14] successfully modeled the complete CLOU process in ASPEN Plus based on a series of detailed experiments. The results from their model were in excellent agreement with the experiments for the flue stream contents of the reactors, oxygen carrier conversion kinetics, and the overall performance of the CLOU process. Scaled-up cases were also conducted to investigate the influence of increase in the coal and oxygen carriers feeding rates. Different types of coals were also investigated to determine their effect on the CO_2 concentration in the flue stream and on the overall energy. This previous work of Zhou et al. [14] has formed the basis for modeling of the CLOU process in this chapter.

In this chapter, we first present the model of CLOU process in ASPEN Plus and compare the simulation results with the data in the recent experiments on CLOU process. After the validation, additional simulations are performed using ASPEN Plus. These include the use of three different types of coal to determine their effect on the overall energy output, and the effect of varying the air flow rate on energy output and the performance of three – Copper (Cu), Manganese (Mn) and Cobalt (Co) based oxygen carriers in the CLOU process.

3.2 Brief Description of the CLOU Experimental Apparatus and Results (Abad et al [2])

A CLOU test apparatus, directly utilizing solid coal as the fuel, with a 1.5kWth output was recently built by Abad et al [2]. A schematic of the CLOU apparatus is shown in Figure 3.1. The experimental set-up basically consists of two interconnected fluidized-bed reactors joined by a loop seal, a cyclone for gas-solid separation for transport of only solid from the air reactor to the fuel reactor, and a valve to control the circulation of solid flow rate in the system. To the authors' knowledge, this experiment is the first time that the CLOU process has been demonstrated in an experiment utilizing two interconnected fluidized-bed reactors using a solid fuel. The solid fuel used in the experiment is a bituminous Colombian coal "El Cerrejon" [2] which is the same as Bituminous coal used in Chapter 2. It should be noted that the coal is subjected to a thermal pre-treatment for pre-oxidation in order to avoid coal swelling and bed agglomeration. Coal was heated at 180 ºC in the atmospheric air for 28 hours. Proximate and ultimate analyses of the pre-treated

coal are given in Table 3.1. Both the experiments and the ASPEN Plus simulations are based on this pre-treated coal. The coal particle size used for this study is 200 to 300 μm. Oxygen carrier particles are prepared by spray drying, containing 60% wt. CuO and use 40% wt. $MgAl_2O_4$ as supporting material. The inclusion of supporting material is to increase the reactivity, durability, and fluidizability of the oxygen carrier [15]. The particle size of the oxygen carrier varies between 100 to 200 μm. The effect of operating conditions on the combustion and CO_2 capture efficiencies are investigated.

Table 3.1 Properties of bituminous Colombian coal "El Cerrejon"

Components	Proximate Analysis (wt. %)				Ultimate Analysis (wt. %)						Energy
	Moisture	Volatile matter	Fixed carbon	Ash	C	H	N	S	O	Ash	LHV (kJ/kg)
Fresh	7.5	34.0	49.9	8.6	70.8	3.9	1.7	0.5	7.20	15.9	25880
Pre-Treated	2.3	33.0	55.9	8.8	65.8	3.3	1.6	0.6	17.6	11.1	21899

The oxygen carrier decomposes in the fuel reactor, exhausting gaseous oxygen to the surroundings. The oxygen burns the volatiles and char produced from coal pyrolysis in the fuel reactor. The re-oxidation of the oxygen carrier takes place in the air reactor, consisting of a bubbling fluidized bed followed by a riser. N_2 and unreacted O_2 leave the air reactor passing through a high-efficiency cyclone and a filter before the stack.

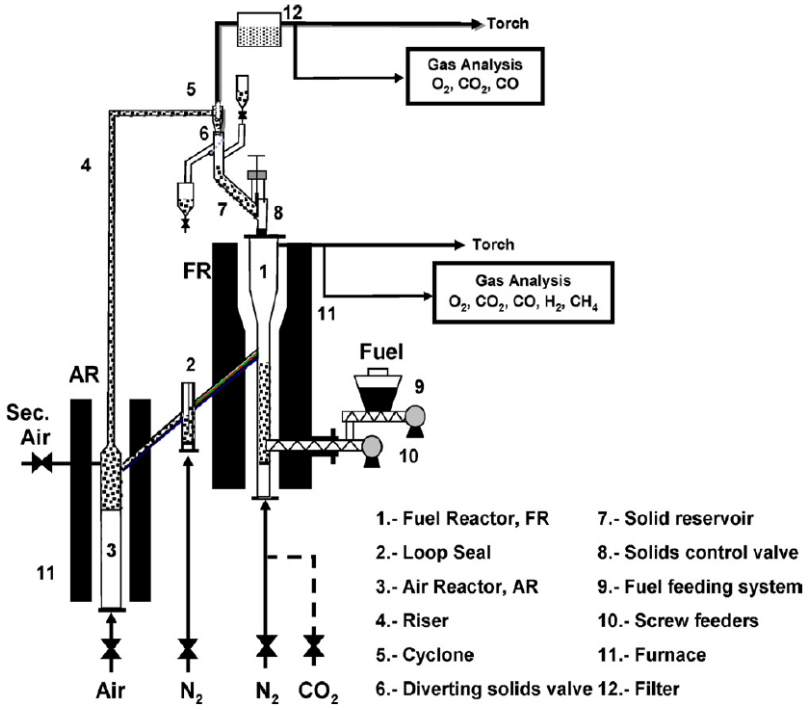

Figure 3.1 Schematic view of the apparatus used in Abad et al.'s experiment [2]

In Abad et al.'s experiment [2], a series of tests were conducted using the same oxygen-carrier. From the experiments, the series of tests with different coal feeding mass were selected for validation of the process simulation in Aspen Plus. Table 3.2 summarizes the details of the experimental operational parameters and the results obtained from the experiments.

Table 3.2 Operational parameters used in Abad et al.'s experiment [2]

Test No.	T_{FR}(℃)	φ	λ	$\dot{m}_s$ (kg/h)	$\dot{m}_{coal}$ (g/h)	Power (W)
CLOU1	924	4.3	4.7	9.0	67	410
CLOU2	929	3.2	3.5	9.0	89	541
CLOU3	917	2.6	2.8	9.0	112	681
CLOU4	920	2.1	2.3	9.0	135	821
CLOU5	925	1.1	1.2	9.0	256	1560

3.3 Process Simulations in ASPEN Plus

As mentioned before, ASPEN Plus is a process simulation software which uses basic engineering relationships such as mass and energy balances and multi-phase and chemical reaction models in modeling a process at system level. It consists of flow sheet simulations that calculate stream flow rates, compositions, properties and operating conditions. For the study of CLOU process, ASPEN Plus can be employed for designing and sizing the reactors, for predicting the reaction conversion efficiency, and for understanding the reaction equilibrium behavior. For validation of CLOU process using ASPEN Plus, we simulate the experiment conducted by Abad et al. [2]. The ASPEN Plus flow sheet model corresponding to the experiment of Abad et al.'s [2] is shown in Figure 3.2.

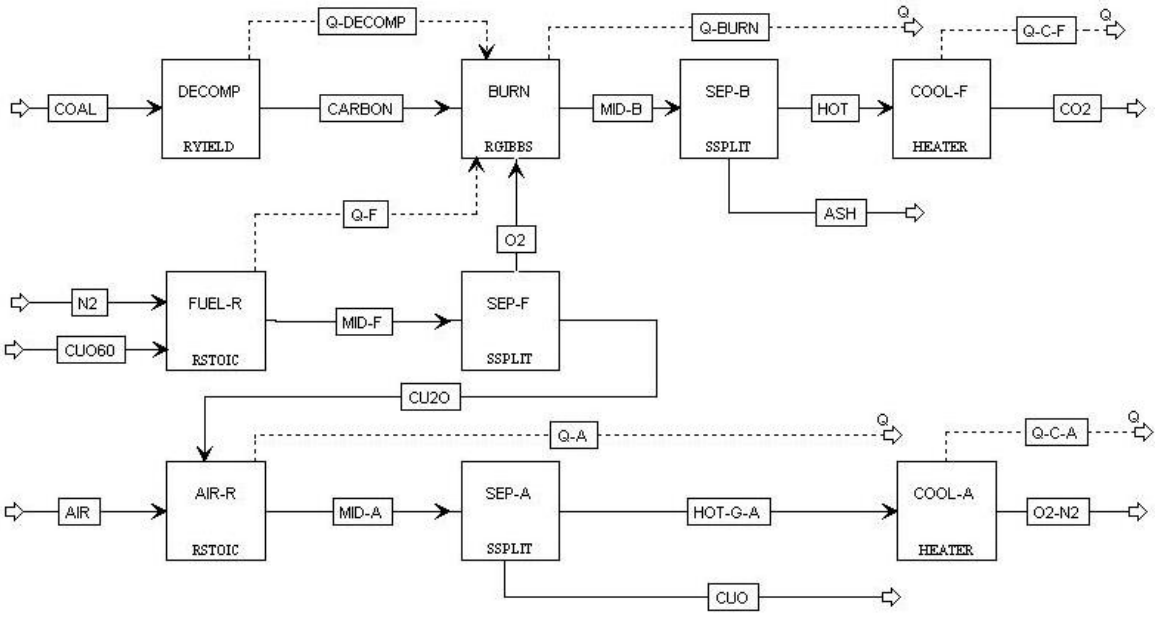

Figure 3.2 The flow sheet of CLOU process in ASPEN Plus

As shown in Figure 3.2 and summarized in Table 3.3, in ASPEN Plus coal devolatilization is defined by the RYIELD reactor, followed by the gasification of coal represented by the RGIBBS reactor. The RSTOIC reactor defines the actual fuel combustion. It should be noted here that these three reactor blocks together represent the fuel reactor in Abad et al.'s experiments [2]. The flow sheet within the ASPEN Plus simulation package cannot model this entire reaction with one reactor. As a result, the fuel reactor is divided into several different reactor simulations. The air reactor is modeled as a RSTOIC reactor. The molar flow rates of CuO exiting and Cu_2O feeding in the RSTOIC

reactor is defined in two separate blocks in the flow sheet in Figure 3.2; these rates are identical and represent the circulation of oxygen Carrier (OC) within the system. It should be noted that the circulation of OC cannot be defined explicitly in the ASPEN Plus model.

Table 3.3 Process models used in different parts of CLOU process in ASPEN Plus

Name	Model	Function	Reaction formula
DECOMP	RYIELD	coal devolatilization and gasification	coal → volatile matter + char
BURN	RGIBBS	syngas and char burn with O_2	char +volatile matter + O_2 → CO_2+ H_2O
FUEL-R	RSTOIC	carrier reduction reaction	$4CuO \rightarrow 2Cu_2O+O_2$
AIR-R	RSTOIC	carrier oxidation reaction	$2Cu_2O+O_2 \rightarrow 4CuO$
SEP-F	SSPLIT	O_2 and Cu_2O separation	~
SEP-A	SSPLIT	CuO and air separation	
SEP-B	SSPLIT	separation - ash and flue gas	
COOL-F	HEATER	flue gas cooler, fuel reactor	$H_2O(gas) \rightarrow H_2O(liquid)$
COOL-A	HEATER	flue gas cooler, air reactor	~

3.4 Validation of the CLC Process Simulation with Experiment

ASPEN Plus model for CLOU process is validated against the experimental data of Abad et al. [5]. Since the focus of this charpter is primarily on energy output from various types of coals using varying air flow rates and different oxygen carriers, only a few CLOU process validation results against the experiment of Abad et al. [2] are presented; in particular the comparison of overall power output between the simulation and the experiment is given. Additional validation results (flue gas concentration, oxygen carrier efficiency etc.) can be found in the paper by Zhou et al. [14]. Figure 3.3 compares the thermal power output of CLOU employed in the experiment in Reference [2] with the simulations reported in Reference [14]. It can be seen from this figure that the overall power output determined by the ASPEN Plus model is in reasonably good agreement with the experimental values for different coal feeding rates. The small differences between the simulations and the experimental results can be attributed to the inability of ASPEN Plus to account for the inevitable losses that occur at multiple locations in the experimental apparatus; the ASPEN Plus

system modeling software neglects miscellaneous energy losses in the system due to changes in the hydrodynamic characteristics. To account for the changes in the hydrodynamics characteristics, detailed hydrodynamic simulations are needed using the computational fluid dynamics software.

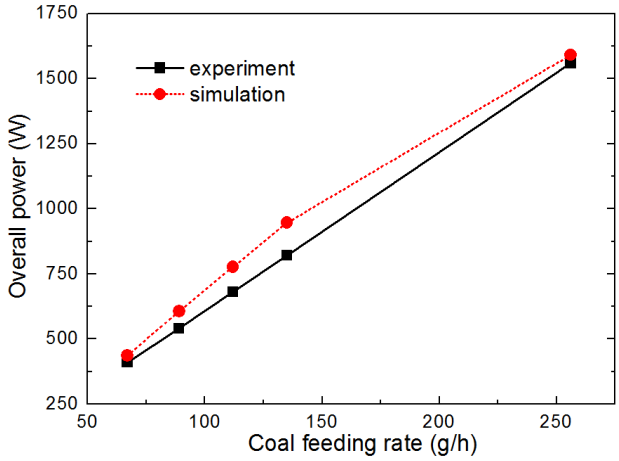

Figure 3.3 Comparison of overall power output comparison between the simulation and the experiment [14]

Table 3.4 summarizes the breakdown of power output for various components of the modeled CLOU system in ASPEN Plus. Energy is consumed mainly in the compressor processes. Compressed air is required in the air reactor to regenerate CuO from Cu_2O. Another compressor is used to compress the steam for the gasifier. There is large amount of energy produced in the air reactor, but the fuel reactor needs to be supplied with energy. This is because the net heat work in the fuel reactor is the summation of the heat work from the DECOMP, BURN, and FUEL-R blocks in Figure 3.2. Although BURN produces energy because of the combustion of syngas, the energy requirement of FUEL-R is more than the energy produced in DECOMP and BURN.

Table 3.4 Thermal analysis at various locations of the modeled CLOU system in ASPEN Plus

Test No.	Total Power (W)	Q-A (W)	Q-Burn (W)	Q-C-A (W)	Q-C-F (W)	Q-Decomp (W)	Q-F (W)
CLOU1	436.6	-175.1	116.4	380	115.3	31.6	-380.1
CLOU2	606.4	-79.9	181.9	370.1	134.3	41.7	-477.6
CLOU3	777.6	-30.5	296.1	361.1	150.8	53.5	-534.5
CLOU4	946.5	51.5	372.7	352.3	170	64.2	-628.8
CLOU5	1591.4	180.3	803.6	338.2	269.3	120.7	-1094

3.5 Effect of Varying the Air Flow Rate on Energy Output Using Different Types of Coal and Oxygen Carriers

The recent paper of Mukherjee et al. [13] suggests that it is favorable to operate the air reactor of the chemical looping combustion (CLC) process at higher temperatures with excess air supply in order to achieve greater power efficiency. Since CLC and CLOU are very similar processes, therefore it is of interest to investigate the effect of air flow rate in the air reactor on the energy output in the CLOU process. In addition it is also of interest to investigate the influence of different OCs on energy output. We consider three types of OCs namely the CuO/Cu_2O, Mn_2O_3/Mn_3O_4, and Co_3O_4/CoO in the simulations. In case of Mn_2O_3/Mn_3O_4 and Co_3O_4/CoO, the oxygen is released according to the following reversible reactions:

$$6\ Mn_2O_3 \rightleftarrows 4\ Mn_3O_4 + O_2 \tag{3.3}$$

$$2\ Co_3O_4 \rightleftarrows 6\ CoO + O_2 \tag{3.4}$$

We also consider three different types of coals, namely the Bituminous, Anthracitic, and Lignite. The detailed properties of these three types of coals are summarized in Table 3.5.

Table 3.5 Properties of three types of coals

Coal name	Proximate Analysis (wt. %)				Ultimate Analysis (wt. %)						Energy
	Moisture	Volatile matter	Fixed carbon	Ash	C	H	N	S	O	Ash	LHV (kJ/kg)
Bituminous	2.3	33.0	55.9	8.8	65.8	3.3	1.6	0.6	17.6	11.1	21899
Anthracite	1.0	7.5	59.9	31.6	60.7	2.1	0.9	1.3	2.4	32.6	21900
Lignite	12.6	28.6	33.6	25.2	45.4	2.5	0.6	5.2	8.5	37.8	16250

3.5.1 Effect of Air Flow Rate on Energy Output Using Three Different Coals with CuO/Cu_2O as OC

In order to evaluate the effect of air flow rate, we keep the amount of coal feeding rate and OC fixed. CuO/Cu_2O is employed as OC for the three types of coals considered in section 3.4. Figure 3.4 shows the trend in power output with increasing air flow rate. Table 3.6 summarizes the power output using three types of coals with CuO/Cu_2O as OC. It can be noted form Figure 3.4 that power increases rapidly and linearly with increase in air flow rate until the air flow rate reaches an almost optimal value of nearly 1500 l/h for 256 g/h of coal feeding rate, beyond which the increase in power output is very gradual. When the air flow rate is less than the1500 l/h, there is not enough air in the air reactor to re-oxidize the Cu_2O which comes from the fuel reactor. 1500 l/h of air is the exact stoichiometric amount to re-oxidize the Cu_2O completely, which is responsible for releasing the total amount of heat. The reason that the overall power continues to increase albeit very gradually for air flow rate greater than 1500 l/h is that the temperature of air reactor is slightly higher than that of the following heat exchanger (which cools the gas out of the air reactor). Therefore with additional air input, slightly additional energy benefit is obtained. However, it is important to note that in the ASPEN Plus model the focus is entirely on heat energy; it does not take into account the mechanical energy consumed by each block of flow sheet in Figure 3.2, for instance the energy required for blowing the air into the air reactor which may consume a significant amount of mechanical energy. Therefore there is lesser benefit of adding more air in the system beyond the stoichiometric amount of 1600 l/h to re-oxidize the Cu_2O. The result of Figure 3.4 is nevertheless important in estimating the amount of near optimal air flow rate and expected near optimal energy output for a given type of coal and OC. It should also be mentioned that these results scale linearly for higher coal feeding rates because of the assumptions made in ASPEN Plus modeling.

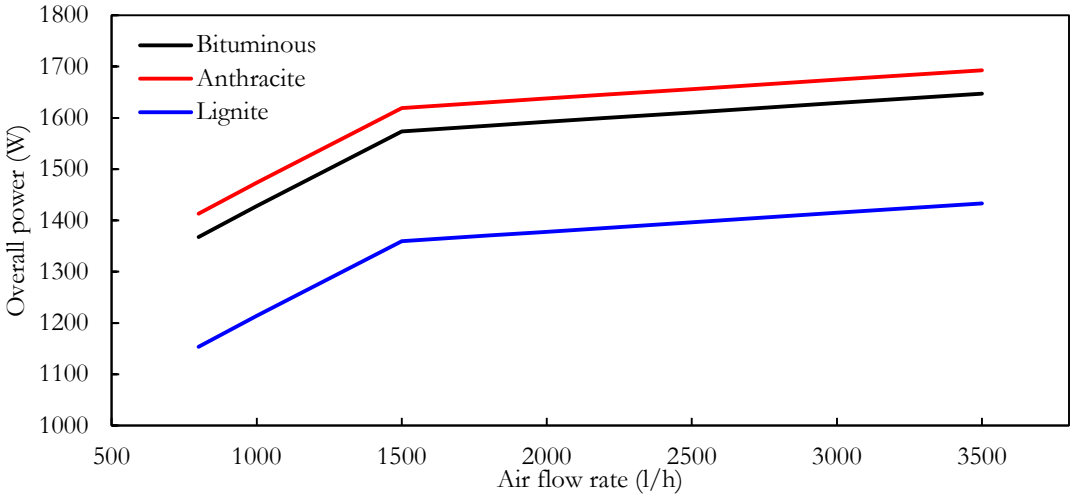

Figure 3.4 Overall energy output with increasing air flow rate using CuO as OC for 256 g/h of coal feeding rate

Table 3.6 Power output from three types of coal with increasing air flow rate using CuO as OC with coal feeding rate of 256 g/h

Coal name	Air flow rate (l/h)								
	800	1000	1500	1800	1980	2200	2500	3000	3500
	Energy output (W)								
Bituminous	1367.6	1428.2	1573.7	1584.7	1591.3	1599.5	1610.5	1628.9	1647.3
Anthracite	1413.3	1473.8	1619.4	1630.4	1637.0	1645.1	1656.2	1674.6	1693.0
Lignite	1153.4	1214.0	1359.5	1370.6	1377.2	1385.3	1396.3	1414.7	1433.1

3.5.2 Effect of Air Flow Rate on Energy Output Using Three Different Coals with Different OCs

Using different OCs, namely the Co_3O_4/CoO and Mn_2O_3/Mn_3O_4, the effect of varying the air flow rate is similar to that shown in Figure 3.4 using CuO/Cu_2O as an OC as shown in Figures 3.5 and 3.6 respectively. The optimal air flow rates are however 1500 l/h and 1800 l/h with Co_3O_4/CoO and Mn_2O_3/Mn_3O_4 as OC respectively. Tables 3.7 and 3.8 summarize the power output for three types of coal using Co_3O_4/CoO and Mn_2O_3/Mn_3O_4 as OC respectively

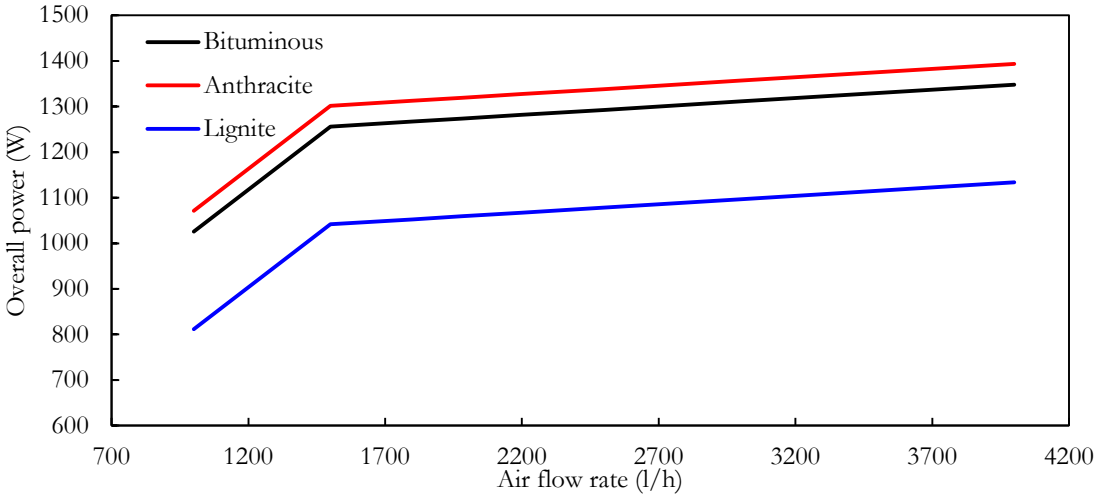

Figure 3.5 Overall energy output with increasing air flow rate using Co_3O_4 as OC for 256 g/h of coal feeding rate

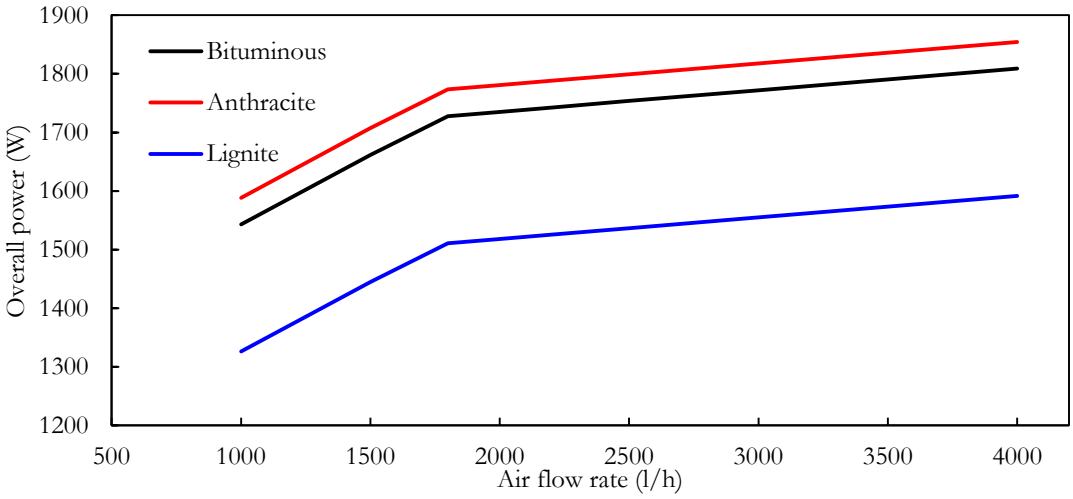

Figure 3.6 Overall energy output with increasing air flow rate using Mn_2O_3 as OC for 256 g/h of coal feeding rate

Table 3.7 Power output from three types of coal with increasing air flow rate using Co_3O_4 as OC with coal feeding rate of 256 g/h

Coal name	Air flow rate (l/h)							
	1000	1500	1800	1980	2200	2500	3000	4000
	Energy output (W)							
Bituminous	1025.4	1255.8	1266.8	1273.4	1281.5	1292.6	1311.0	1347.8
Anthracite	1071.1	1301.4	1312.4	1319.1	1327.2	1338.2	1356.6	1393.4
Lignite	811.3	1041.6	1052.6	1059.3	1067.4	1078.4	1096.8	1133.6

Table 3.8 Power output from three types of coal with increasing air flow rate using Mn_2O_3 as OC with coal feeding rate of 256 g/h

Coal name	Air flow rate (l/h)							
	1000	1500	1800	1980	2200	2500	3000	4000
	Energy output (W)							
Bituminous	1543.0	1661.5	1727.8	1734.4	1742.5	1753.5	1771.9	1808.8
Anthracite	1588.6	1707.1	1773.4	1780.0	1788.1	1799.2	1817.6	1854.4
Lignite	1326.1	1444.6	1510.9	1517.5	1525.6	1536.7	1555.1	1591.9

Next we consider the Case #5 – CLOU5 in Table 3.2. Keeping the amount of coal feeding rate to be the same at 256 g/h, we compare the maximum power output in Table 3.9 using the optimal air flow rate and three different OCs with varying amount for three different types of coal. The heat of various components in CLOU model of each case is summarized in Table B.1 – B.9. It turns out that the amount of OC required for maximum power output is different depending upon its type. The amount of OC required varies as $Mn_2O_3 > CuO > Co_3O_4$ (the exact amounts are given in Table 3.9). This variation in the OC amount occurs due to the chemical reaction property of various OCs described below.

Table 3.9 Comparison of maximum power output from three different types of coal using optimal air flow rate and optimal amounts of three different OCs

Coal type and amount	OC type	OC amount (kg/h)	Optimal air flow rate (l/h)	Maximum power output (W)
Bituminous - 256 g/h	CuO	9	1500	1573.71
	Co_3O_4	13.5	1500	1255.75
	Mn_2O_3	26	1800	1727.77
Anthracite - 256 g/h	CuO	9	1500	1619.39
	Co_3O_4	13.5	1500	1301.40
	Mn_2O_3	26	1800	1773.39
Lignite - 256 g/h	CuO	9	1500	1359.54
	Co_3O_4	13.5	1500	1041.59
	Mn_2O_3	26	1800	1510.89

In the case of Copper and Manganese oxides, the overall reaction with carbon is exothermic in the fuel-reactor as shown in equations (3.5) and (3.6). On the other hand the reaction of the Cobalt oxide with carbon is an endothermic reaction as shown in equation (3.7) [2].

$$4CuO + C \rightarrow 2Cu_2O + CO_2 \qquad \Delta H_r^{900°C} = -132.9 \text{ kJ/mol } O_2 \tag{3.5}$$

$$6Mn_2O_3 + C \rightarrow 4Mn_3O_4 + CO_2 \qquad \Delta H_r^{900°C} = -201.9 \text{ kJ/mol } O_2 \tag{3.6}$$

$$2Co_3O_4 + C \rightarrow 6CoO + CO_2 \qquad \Delta H_r^{900°C} = 11.7 \text{ kJ/mol } O_2 \tag{3.7}$$

3.6 Conclusion

In this chapter, ASPEN Plus software is employed to model and study the CLOU process. The ASPEN Plus simulations are validated using information from a series of test cases conducted in a

CLOU experiment [2]. Excellent agreement is obtained between the simulations and the experimental results for power output. It is demonstrated that the ASPEN Plus can provide a creditable process simulation platform for the study of CLOU process. More detailed validation results can be found in Zhou et al [14]. It is shown that the coal rank has significant impact on overall energy release; the Bituminous coal and Anthracitic coal show similar and better CLOU process performance compared to the Lignite coal. The similarity in the CLOU process performance of Bituminous coal and Anthracitic coal can be explained by the fact that both have similar carbon content. The results indicate that the char gasification is not a very significant factor in CLOU process performance since the presence of oxygen enables the solid-gas combustion to take place without gasification. More importantly, the effect of varying the air flow rate on overall energy output is investigated; there exists an optimal air flow rate to obtain the maximum power output for a given coal feeding rate and coal type. The effect of three different oxygen carriers on energy output is also investigated using the optimal air flow rate. Among the three oxygen carriers CuO, Mn_2O_3, and Co_3O_4, the best performance in terms of power output is achieved by Mn_2O_3. The results presented in this paper can be used to estimate the amount of various quantities such as the air flow rate and oxygen carrier (and its type) required to achieve near optimal energy output and CO_2 capture from a CLOU process based power plant.

Chapter 4 Reactor Level CFD Simulations of CLC

4.1 Introduction

After the system level simulations of CLC and CLOU described in Chapter 2 and 3 respectively using ASPEN Plus, next step is to investigate a the CFD simulations of a complete three-dimensional model of the chemical-looping combustion system. In this thesis, a full CLC system of National Energy Technology Laboratory (NETL) is modeled in three dimensions using the ANSYS Fluent [16, 17] hydrodynamic model with the discrete element method (DEM). A CFD simulation for this case has alse been conducted by Parker [3] using the Barracuda software (CFPD Software, LLC, Albuquerque NM).

For developing a credible CFD simulation of an interconnected dual circulating fluidized bed configuration of a CLC setup, it requires of accurate modeling of multiphase fluid flow involving gas and particles. As discussed in the paper of Zhang et al [18], there are two approaches to address the simulation of solid-gas coupled multiphase flow. One approach is to assume that the particulate phase is also in continuum and thus can be treated as a secondary but heavier "gas" phase. Because the fluid-based mass and momentum equations are solved for both phases within the Eulerian framework, this approach is also known as the multiphase Eulerian method or the granular flow method. In the second approach, the particulate phase is modeled at individual particle level tracking their movement using the Lagrangian framework and is coupled with the fluid field for interphase mass and momentum exchange. Because the particles are treated as discrete elements, this approach is also known as the discrete-element method (DEM). The typical interconnected fluidized bed configuration of CLC and the presence of solid fuel in it require the capability of accurate capture of the solids circulation and separation in the system. Therefore, the consideration of solid-gas two-way coupling and solid-solid interaction becomes important in these simulations.

In this chapter, a series of transient simulations of 3D fluidized bed apparatus for CLC process at NETL [3] are performed using the CFD/DEM coupled model. The tracking of individual solid particles in time and their interaction with each other as well as with the ambient fluid is enabled to provide an accurate and realistic representation of the multiphase flow field. The modeling of chemical reactions is not considered in this thesis; it will be addressed in future work.

4.2 Modeling Approach

This work employs the commercial CFD simulation package ANSYS Fluent, release version 15.0 [16, 17]. In the coupled CFD/DEM approach to multiphase simulation of CLC process, the fluid motion is computed by solving the incompressible continuity and Navier–Stokes equations. The motion of solid particles is modeled by the Newtonian equation of motion. The CFD/DEM approach tracks each particle in the system individually and considers its position, velocity and its interaction with other particles and walls. The overall behavior of the system is a result of the interaction of all individual particles among themselves and with the surrounding gas phase. In order to achieve a coupled CFD/DEM simulation for multiphase flow, source terms are introduced in the Navier–Stokes equations to capture the solid-gas momentum exchange and in the Newtonian equations of motion to account for the forces due to the fluid on the solid particles. Details of the equations used to compute the fluid and motion of solid particles are provided in the following sections.

4.2.1 Fluid Equations

To account for the presence of the solid particles, the equations of fluid motion are slightly modified. This is done by including the porosity which is defined to be equal to the volume fraction of the fluid α_f in the computational cell to which the equations are applied. Furthermore, source terms are added in the equation to account for the transfer of momentum. Thus, the volume-averaged continuity equation and Navier–Stokes equations for CFD/DEM simulation can be written as:

$$\frac{\partial}{\partial t}\left(\alpha_f \rho_f\right) + \nabla \cdot \left(\alpha_f \rho_f \boldsymbol{u}_f\right) = 0 \tag{4.1}$$

$$\frac{\partial}{\partial t}\left(\alpha_f \rho_f \boldsymbol{u}_f\right) + \nabla \cdot \left(\alpha_f \rho_f \boldsymbol{u}_f \boldsymbol{u}_f\right) = -\alpha_f \nabla p_f - \nabla \cdot \bar{\bar{\tau}}_f + \alpha_f \rho_f \boldsymbol{g} - \boldsymbol{K}_{sg} \tag{4.2}$$

where ρ_f, $\boldsymbol{u}_f$, p_f are the density, velocity and pressure of the fluid respectively; $\boldsymbol{g}$ is the acceleration due to gravity. The source term in the momentum equation, $\boldsymbol{K}_{sg}$ is used to couple the solid and gas phases by accounting for the solid-gas momentum exchange from the interphase drag due to the presence of the solid particles. For Newtonian fluid such as air or gaseous CO_2, the viscous shear tensor of fluid τ_f can be written as:

$$\bar{\bar{\tau}}_f = \mu_f\left(\nabla \boldsymbol{u}_f + \nabla {\boldsymbol{u}_f}^T\right) + (\lambda_f + \frac{2}{3}\mu_f)\nabla \boldsymbol{u}_f \bar{\bar{I}} \tag{4.3}$$

where μ_f is the fluid viscosity.

4.2.2 Particle Equations

In the CFD/DEM simulation, each solid particle is tracked individually. The motion of each solid particle is obtained by summing the forces acting on the particle and applying Newton's second law of motion. The resulting force balance equation, which is integrated to obtain the motion of the solid particle, is given by

$$m_s \frac{d\boldsymbol{u}_s}{dt} = \sum \boldsymbol{F}_i = \boldsymbol{F}_{\text{gra}} + \boldsymbol{F}_{\text{buo}} + \boldsymbol{F}_{\text{drag}} + \boldsymbol{F}_{\text{pre}} + \boldsymbol{F}_{\text{Saf}} + \boldsymbol{F}_{\text{Mag}} + \boldsymbol{F}_{\text{con}} \tag{4.4}$$

where $\boldsymbol{F}_{\text{gra}}$ and $\boldsymbol{F}_{\text{buo}}$ are bulk forces due to gravity and buoyancy, respectively; $\boldsymbol{F}_{\text{drag}}$, $\boldsymbol{F}_{\text{pre}}$, $\boldsymbol{F}_{\text{Saf}}$, $\boldsymbol{F}_{\text{Mag}}$ are hydrodynamic forces due to momentum transfer between the solid particles and surrounding fluid, namely, the drag force due to fluid viscosity, the pressure force due to pressure gradient, Saffman lift force due to interparticle friction, and the Magnus force due to particle spin, respectively. Because of the large difference between the solid particle density and fluid density, the pressure force can be dropped from equation (4.4) without loss of accuracy; the Magnus force can also be dropped due to negligible particle rotation. $\boldsymbol{F}_{\text{con}}$ is the contact force on the particles due to collision with other particles or walls. In this thesis, this contact force is computed using the soft-sphere model, which decouples its normal and tangential components [17]. The normal force on any particle involved in a collision is given by

$${\boldsymbol{F}^n}_{\text{con}} = (k\delta + \gamma(\boldsymbol{u}_{12}\boldsymbol{e}))\boldsymbol{e} \tag{4.5}$$

wher k e is the spring constant of the particle, δ is the overlap between the particle pair involved in the collision, γ is the damping coefficient, $\boldsymbol{u}_{12}$ is the relative velocity vector of the colliding pair, and $\boldsymbol{e}$ is the unit vector. Previous research has demonstrated that for large values of k, the results with the soft-sphere model are interchangeable with those obtained using a hard-sphere model [19]. The tangential contact force is calculated based on the normal force as

$$\boldsymbol{F}^{t}{}_{\text{con}} = \mu \boldsymbol{F}^{n}{}_{\text{con}} \tag{4.6}$$

where μ is the coefficient of friction and is a function of the relative tangential velocity $\boldsymbol{v}_r$ given as

$$\mu(v_r) = \begin{cases} \mu_{\text{stick}} + (\mu_{\text{stick}} - \mu_{\text{glide}})\left(\frac{v_r}{v_{\text{glide}}} - 2\right)\left(\frac{v_r}{v_{\text{glide}}}\right) & if\ v_r < v_{\text{glide}} \\ \mu_{\text{glide}} & if\ v_r \geq v_{\text{glide}} \end{cases} \tag{4.7}$$

The contact force of a collision pair is evaluated as shown in the Figure 4.1.

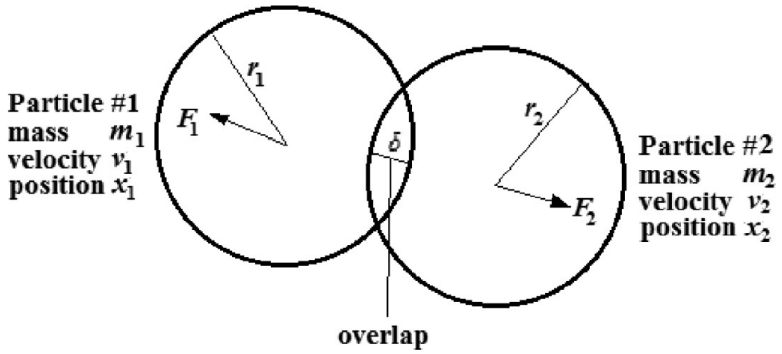

Figure 4.1 Schematic of particle collision model for DEM

4.2.3 Solid-Gas Momentum Exchange

It is vital to evaluate the momentum exchange between the solid and fluid phase for multiphase flow modeling using the coupled CFD/DEM solver; this is done by considering the drag force. The transfer of momentum from the fluid to a solid particle as it moves through each cell in the computational domain is attributed to the drag force exerted on the particle by the fluid, and is modeled as

$$\boldsymbol{F}_{\text{drag}} = F_D(\boldsymbol{u}_f - \boldsymbol{u}_p) \tag{4.8}$$

where $\boldsymbol{u}_f$ is the fluid velocity, $\boldsymbol{u}_p$ is the particle velocity, and F_D is the net drag coefficient. The net drag coefficient can be obtained from

$$F_D = \frac{18\mu}{\rho_p {d_p}^2} \frac{C_D Re_p}{24} \tag{4.9}$$

where μ, ρ_p, d_p are the viscosity of the gas and the density and diameter of the solid particle, respectively. C_D and Re_p are the particle drag coefficients for a sphere and the relative Reynolds number based on the particle diameter, respectively. Re_p is defined as

$$Re_p = \frac{\rho_f d_p |\boldsymbol{u}_f - \boldsymbol{u}_p|}{\mu} \tag{4.10}$$

The corresponding momentum transfer from the solid phase to the gas phase is incorporated by adding the source term $\boldsymbol{K}_{sg} = \beta_{sg}(\boldsymbol{u}_f - \boldsymbol{u}_p)$ in the momentum equation for the gas phase. β_{sg} is the solid-gas exchange coefficient and is obtained by using the relation

$$\beta_{sg} = \frac{\alpha_p \rho_p}{\tau_p} f \tag{4.11}$$

where α_p is the volume fraction of the solid phase in the cell, τ_p is the particle relaxation time defined as $\tau_p = \rho_p {d_p}^2 / 18 u_f$ and f is the drag coefficient. The drag coefficient can be modeled using various empirical relations. The spherical drag law is chosen for this work.

4.2.4 Parcel Concept

To track each individual particle is extremely computationally demanding in a conventional CFD/DEM approach. The total number of particles increases exponentially as the particle size becomes smaller. For instance, in a lab-scale CLC system, the particle number is around 7×10^{11}, which is far beyond the capacity of current computational resources [20]. Therefore, the parcel methodology proposed by Patankar [21] is employed in this thesis to overcome this problem.

According to the parcel concept, one parcel of particles can represent a group of particles with the same properties (e.g. size and density). The mass used in collisions is that of the whole parcel rather

than a single particle. By summing the mass and volume of each individual particle, the total mass (m_p) and volume (V_p) of the parcel can be obtained. The radius of the parcel is thus determined by the mass of the entire parcel and the particle density.

For a given point in the fluid flow, the driving force of a parcel due to fluid forces is assumed to be the same as the sum of the fluid force acting on the group of particles it represents:

$$f_{f,p} = \sum_{i=1}^{N_p} f_{f,i} \tag{4.12}$$

where N_p is the number of particles contained in a parcel, and $f_{f,i}$ is the total fluid force acting on a particle "i". The acceleration due to inter-particle collision forces and particle-wall collisions forces are calculated according to the properties of the parcel of particles.

4.3 Geometry and Mesh

NETL geometry is employed in this thesis as given in the paper by Parker [3]. CFD/DEM simulation conducted on this geometry shown in the Figure 4.2, which consists of an air reactor, cyclone, loop seal, fuel reactor and L-valve. The entire geometry is approximately 12 feet high. The particles start from the bottom of the air reactor and rise up along the riser. Then they move horizontally through the pipe and reach the cyclone. In the cyclone, the particles are separated from the air stream and drop into the loop seal due to the gravity. After passing through the slightly fluidized loop seal, the particles move into the fuel reactor. Finally, the particles leaving the fuel reactor pass through an L-valve and return to the air reactor. The dimensions of the various components are given below.

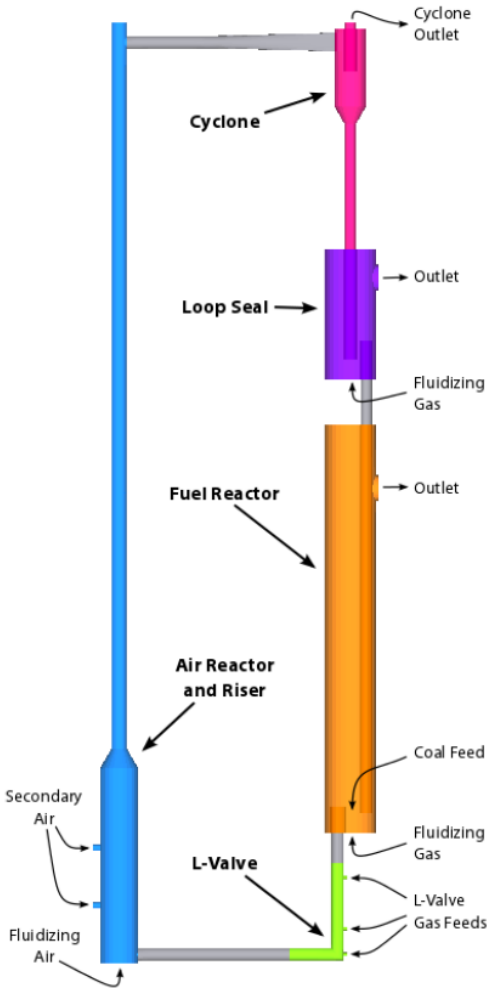

Figure 4.2 Geometry of the chemical-looping combustion system [3]

Air Reactor: The air reactor consists of a 6" diameter, 2.5' tall mixing zone below a 2.5" diameter, 9.5' tall riser. Fluidizing air is injected at the bottom of the air reactor and the secondary air is provided at the locations shown in the Figure 4.2.

Fuel Reactor: The fuel reactor is an 8" diameter, 5' tall cylindrical vessel. Fluidizing nitrogen gas is injected at the bottom of the reactor and a fuel (coal particle or methane gas) is injected either at a coal feed port or with the fluidizing gas (N_2).

Cyclone: The cyclone separates the particles and the gas. Inside the cyclone, the gas exits the cyclone through the outlet located on the top whereas the particles leave the cyclone through the bottom and enter the loop seal.

Loop Seal: The loop seal is a small 8" diameter vessel that is fluidized with nitrogen gas at the bottom and has a gas outlet near the top.

L-valve: The L-valve has three injections of nitrogen gas, which are used to keep particles moving through the horizontal pipe and thereby regulate the circulation rate of the loop.

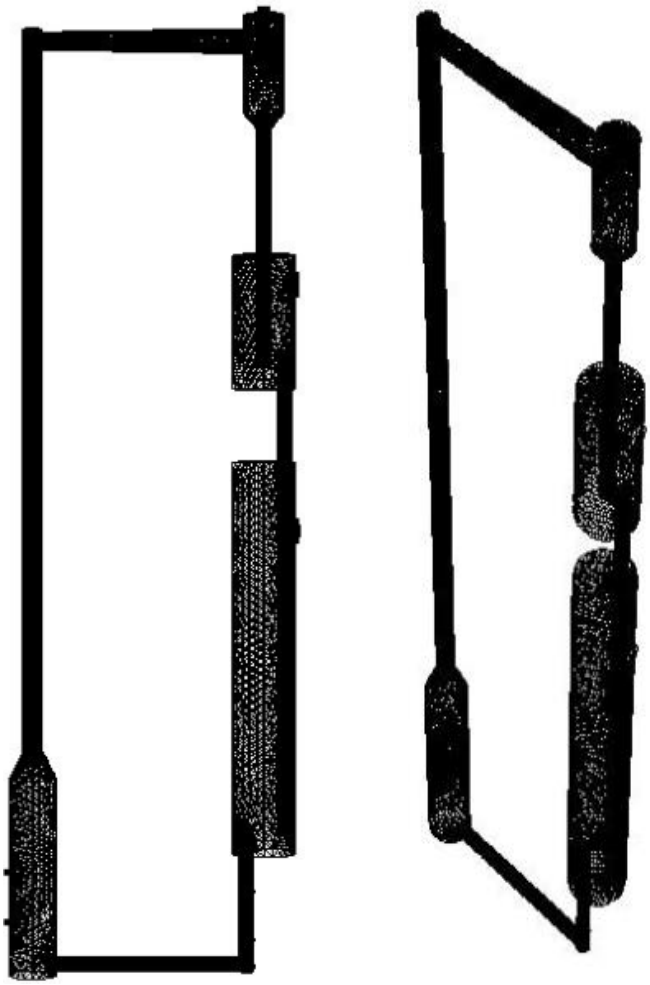

Figure 4.3 Mesh in the chemical-looping combustion system

Based on the geometry, the mesh is generated using ANSYS mesh tool as shown in the Figure 4.3.

4.4 Boundary Conditions and Initial Condition

The boundary conditions for the cold flow simulation have been provided by Parker [3]. The conditions at the flow boundaries and pressure boundaries are summarized in Table 4.1.

Table 4.1 Boundary conditions for cold flow simulation

Flow Boundaries			
Unit	Boundary	Gas	Rate (m/s)
Air Reactor	Fluidizing air	Air	20
	Secondary air (upper)	Air	456.2
	Secondary air (lower)	Air	456.2
Fuel Reactor	Fluidizing gas	N_2	4
Loop Seal	Fluidizing gas	N_2	2
L-valve	Stripper (upper)	N_2	0.5
	Aeration (middle)	N_2	1
	Eductor (lower)	N_2	1
Pressure Boundaries			
Unit	Boundary	Gas	Pressure (kPa)
Fuel Reactor	Outlet	N_2	101.325
Loop Seal	Outlet	N_2	101.325
Cyclone	Outlet	Air	101.325

The initial location of the particles is shown in the Figure 4.4, and the particles are colored by the velocity magnitude. 717,879 particles in total are injected into the whole system. There are 73,360 particles in the air reactor, 365,057 particles in the fuel reactor, and 279,462 particles in the loop seal.

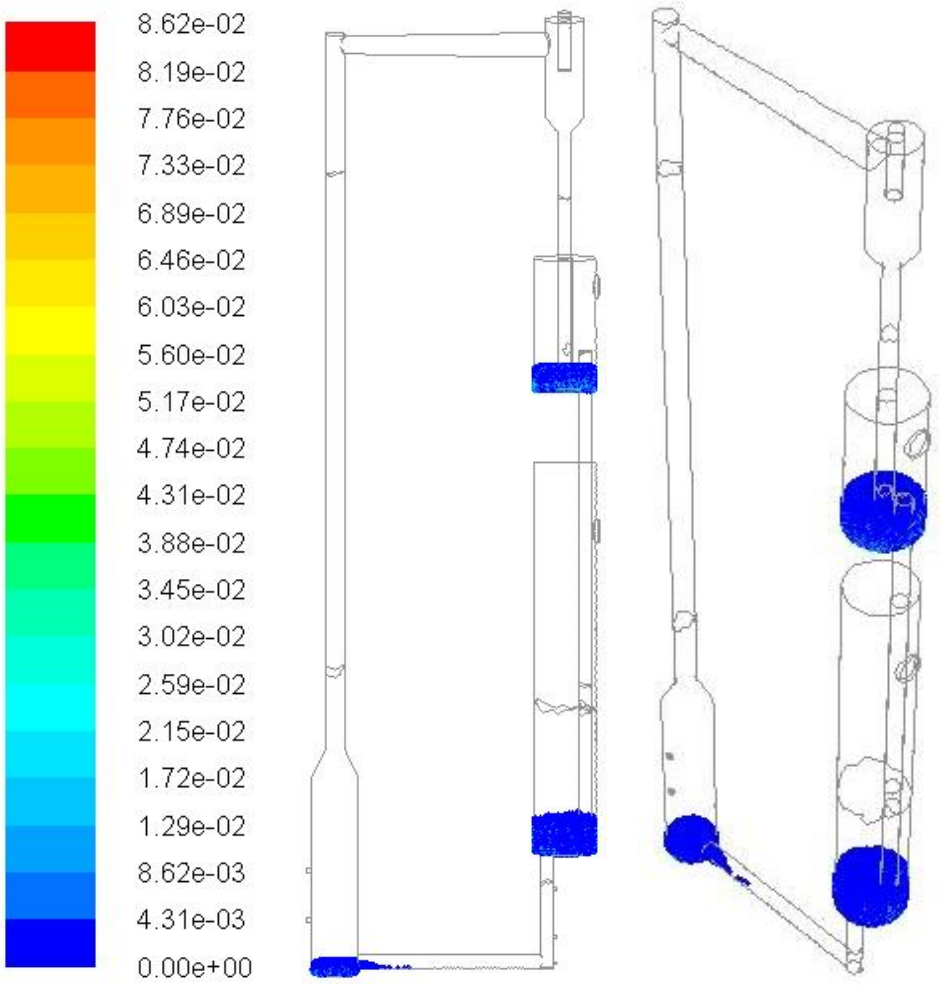

Figure 4.4 Initial particle setup for cold flow simulation

4.5 Cold Flow Simulation Results

The CFD/DEM model is used to simulate 360 ms of cold flow operation including the start up. The results of particle movement are shown in the Figure 4.5, and the particles are colored by velocity magnitude. Particles in the air reactor rise up through the riser, reach the top of the riser at around 190 ms, and then move horizontally along the pipe towards the cyclone. The horizontal movement is driven by the two secondary gas injections on the side of the air reactor. After 40 ms, the particles enter the cyclone and start to drop down to the loop seal due to the gravity. For startup process, particles in the fuel reactor and loop seal are shot up due to the high velocity of gas injection at the bottom of fuel reactor and loop seal. The velocity of gas injection for fuel reactor

and loop seal is reduced to 4 m/s and 2 m/s respectively at 210 ms. From then on, the particles start to settle down.

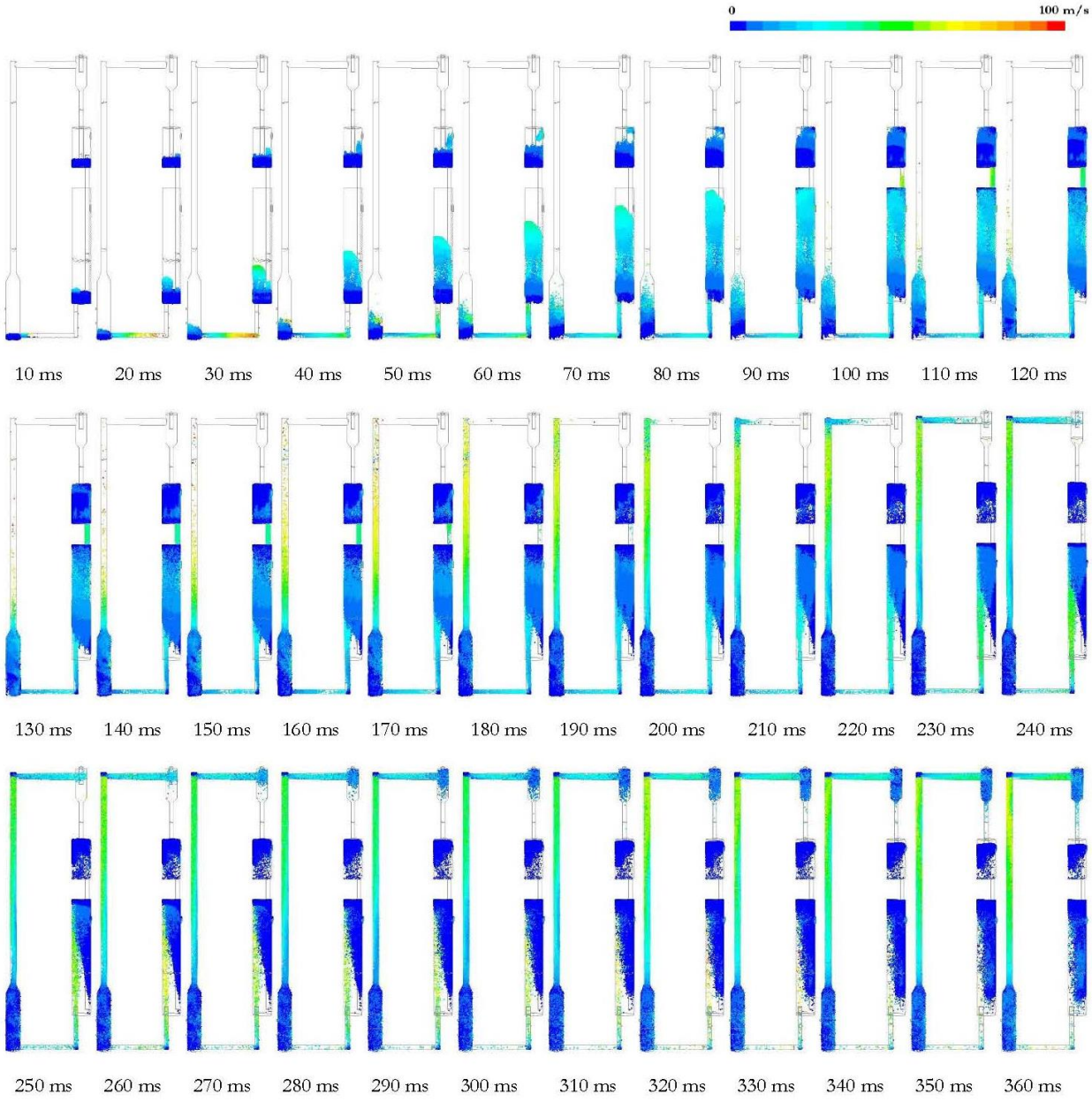

Figure 4.5 Particle movement in the cold flow simulation

360 ms is not an adequate time to see the complete recirculation of the particles. After the particles settle down in the loop seal, they will go through the pipe connected with the fuel reactor and then reach the bottom of the fuel reactor. In the fuel reactor, the particles will drop down to the L-valve,

and due to the additional gas injection in the L-valve, the particles will be pushed back in to the air reactor thus completing the loop. Although these movements do not happen within 360 ms of simulation, the pressure contours and pressure difference at multiple locations of the CLC system provide evidence of the particle recirculation. In Figure 4.6, the system is colored by the gas pressure inside the CLC system. The highest pressure occurs in the air reactor whereas the lowest pressure occurs in the loop seal and the fuel reactor (which have pressure boundaries). After the particles settle down in the fuel reactor, some increase in the gas flow rate in the L-valve needs to be made in order to improve the circulation rate through the loop.

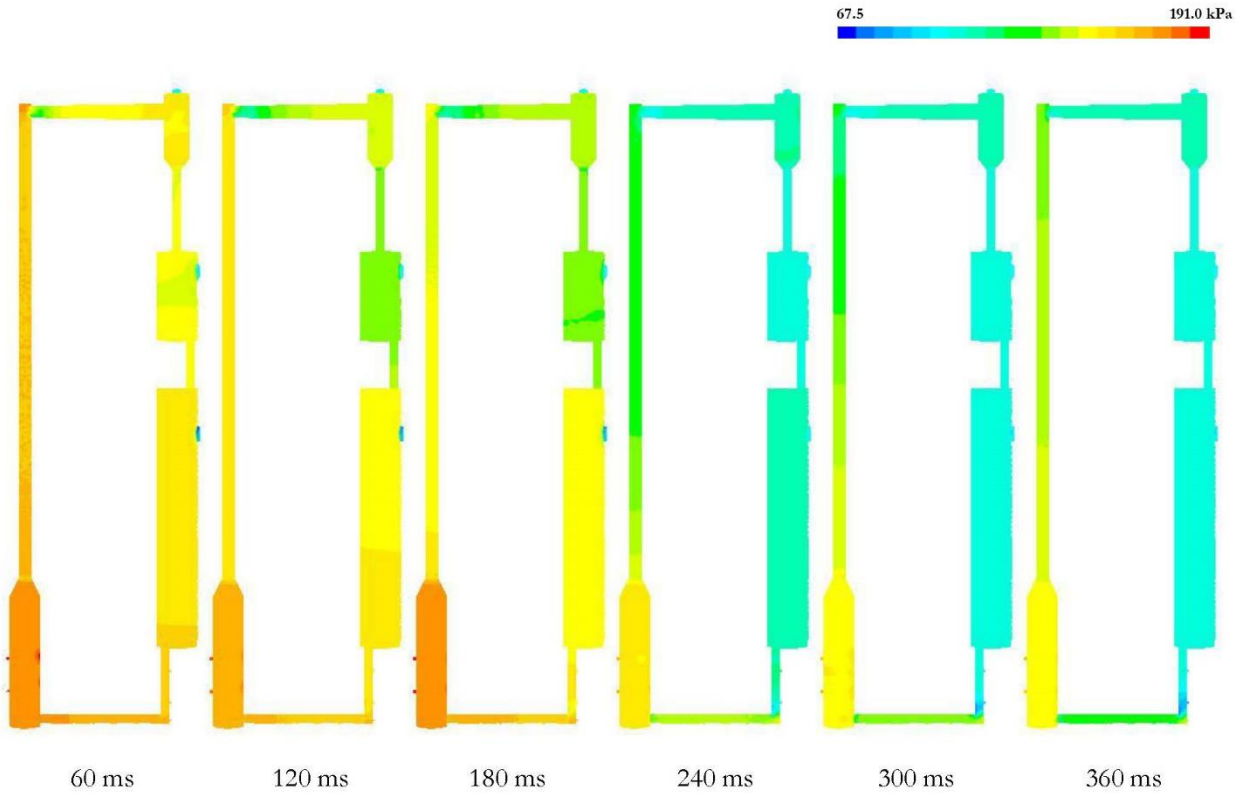

Figure 4.6 Pressure contour for cold flow inside the CLC apparatus

Figure 4.7 shows the CLC system with 6 surfaces that are picked for the interest of investigating the average static pressure. S_1 is in the middle of the air reactor, between the two secondary gas injections; S_2 is located at the top of the riser; S_3 is at the bottom of the cyclone; S_4 and S_5 are respectively on the up and down side of the pipe which connects the loop seal and the fuel reactor;

and S_6 is in the L-valve. S_1-S_5 are the surfaces in the horizontal plane while the S_6 is in the vertical plane.

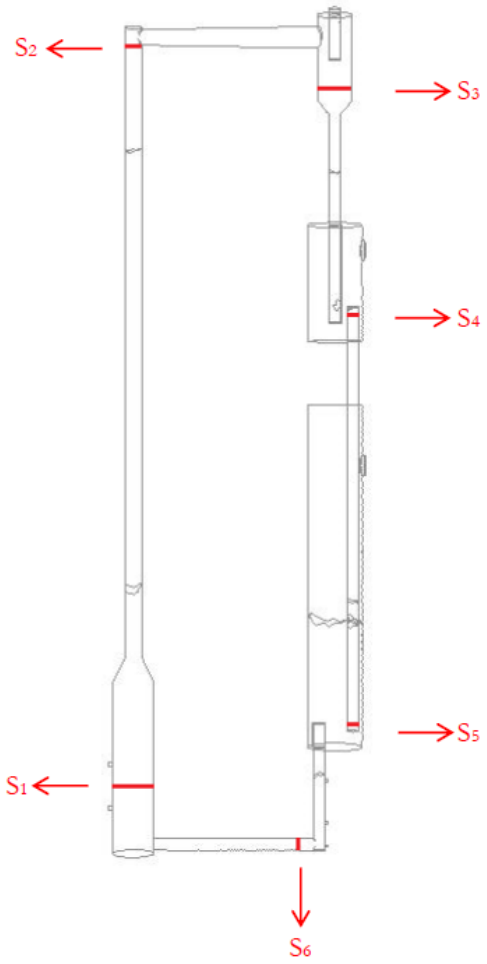

Figure 4.7 Geometry with six pressure surfaces considered

Figure 4.8 shows the static pressure at S_1-S_6 surfaces at different time i.e. at 240 ms, 280 ms, 320 ms and 360 ms. In general, the static pressure doesn't change much during this period of time. Static pressure at S_3-S_6 surfaces decreases slowly; static pressure at S_1 surface decreases during 240 ms to 280 ms, then somewhat increases from 280 ms to 320 ms, and decreases again from 320 ms to 360 ms; static pressure at S_2 surface decreases during 240 ms to 280 ms, and then increases during 240 ms to 360 ms.

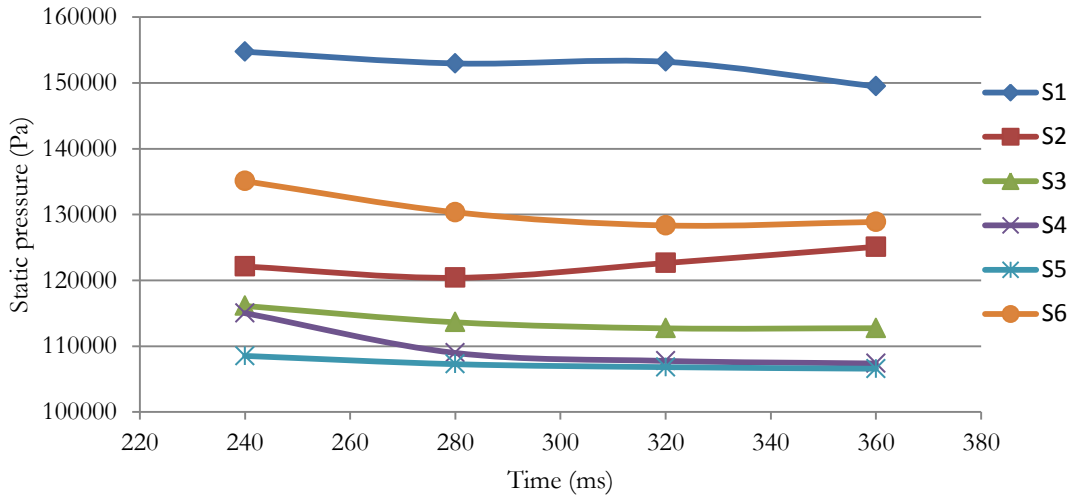

Figure 4.8 Static pressure variation with time at six pressure surfaces S_1-S_6

At 360 ms, pressure difference between various surfaces S_1-S_6 is shown in the Figure 4.9. This figure indicates the particle movement direction. It can be noted that particles move from the fluidized bed (S_1) to the top of the air reactor (S_2) and then to the cyclone (S_3). Pressure of S_4 is greater than that of S_5, which drives the particles from loop seal to the fuel reactor. As for the pressure difference in the L-valve, it can be seen from the right most pressure contour in Figure 4.6, which ensures that the particles can be sent back to the air reactor.

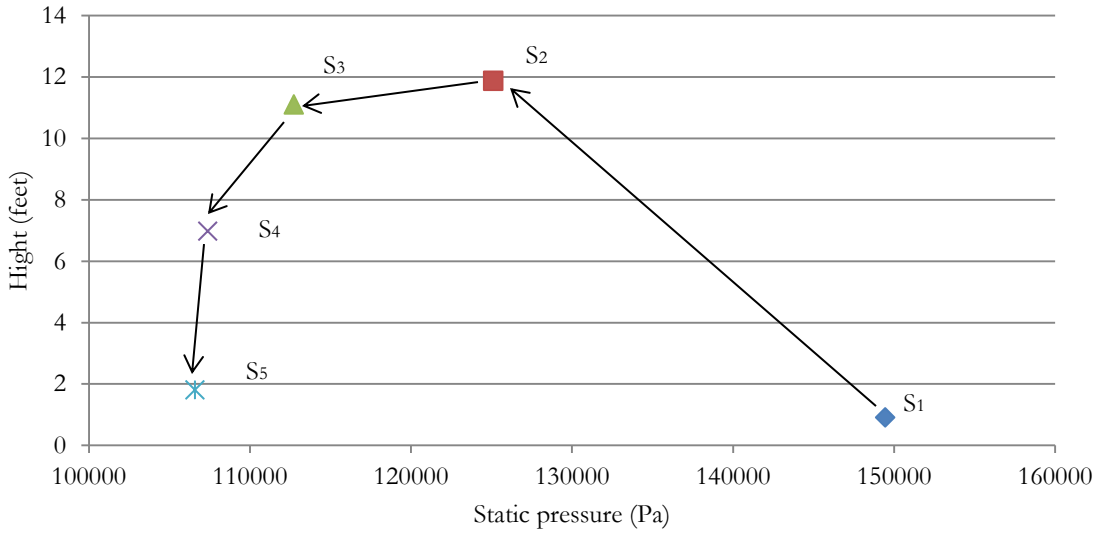

Figure 4.9 Static pressure at S_1-S_5 surfaces at 360 ms

4.6 Conclusion

In this chapter, CFD/DEM coupled multiphase flow simulations of chemical-looping combustion have been performed using ANSYS Fluent CFD package. The reactor level simulation for cold flow is successfully achieved. The geometry proposed by NETL is employed in the model. Velocity and pressure results are obtained from 0 to 360 ms, and particle movement is examined every 10 ms. Although 360 ms is not an enough time to see the complete recirculation, the pressure contours and the pressure difference between S_1-S_5 surfaces in the apparatus provide the evidence of particle recirculation. The cold flow simulation has been designed only for investigating the particle recirculation; in future work, the particle property (e.g. density, size) and chemical reaction need to be taken into account.

Chapter 5 Conclusion

In this thesis, we have successfully conducted two types of simulations (process level and reactor level) of chemical looping combustion (CLC) and chemical looping with oxygen uncoupling (CLOU). Process level simulation results of CLC and CLOU which are both conducted in ASPEN Plus are compared and validated against previous simulation work and experimental data. ASPEN Plus is proven to be capable to model the complete CLC and CLOU processes. In order to obtain the maximum energy output for CLC and CLOU processes, we conducted several more simulations by varying air flow rate and oxygen carrier feeding rate. Through these cases, we calculated the optimal ratio between coal, air flow rate and oxygen carrier amount for the maximum energy output. Different types of coals have different ratios due to their physical and chemical properties. Scaled-up cases also have been run, but the linearity relation between coal feeding rate and energy output is not expected in reality. The reactor level simulation of CLC was conducted in ANSYS Fluent by using the coupled CFD/DEM approach. The modeled CLC apparatus consists of air reactor, cyclone, loop seal, fuel reactor and L-valve. More than 700,000 particles were injected into the system, and each particle was tracked individually in all parts of the apparatus. There is no chemical reaction in the cold flow simulation. Because of the limit of simulation time (360 ms), the particle recirculation had not been complete, but the pressure differences provide the evidence of it.

Appendix A Simulation Results of CLC

Table A.1 CLC process simulation results for different air flow rates with Colombian coal at 100 kg/h and Fe_2O_3/Al_2O_3 at 5921/3951 kg/h

Initial values	Coal (kg/h)	100	100	100	100	100	100
	Water (kg/h)	140	140	140	140	140	140
	Air Flow Rate (kg/h)	100	300	400	500	600	713
	Temperature of Fuel Reactor (ºC)	950	950	950	950	950	950
	Temperature of Air Reactor (ºC)	935	935	935	935	935	935
	Fe_2O_3 flow in the Fuel Reactor (kg/h)	5921	5921	5921	5921	5921	5921
	Al_2O_3 in the System (kg/h)	3951	3951	3951	3951	3951	3951
	Particle Density (kg/m³)	3200	3200	3200	3200	3200	3200
Energy balance (kW)	Fuel Reactor	-161.8	-161.8	-161.8	-161.8	-161.8	-161.8
	Air Reactor	96.498	289.5	386	482.49	578.99	688
	Cool air reactor exhaust	18.996	56.988	75.985	94.981	113.98	135.4
	Cool flue gas	148.3	148.3	148.3	148.3	148.3	148.3
	Cool OC for air reactor	40.9	40.9	40.9	40.9	40.9	40.9
	Reheat OC for fuel reactor	-42.7	-42.7	-42.7	-42.7	-42.7	-42.7
	Heat steam	-69.8	-69.8	-69.8	-69.8	-69.8	-69.8
	Heat air	-25.82	-77.47	-103.3	-129.1	-154.9	-184.1
	Net	4.57	183.92	273.59	363.26	452.93	554.2
Initial values	Coal (kg/h)	100	100	100	100	100	100
	Water (kg/h)	140	140	140	140	140	140
	Air Flow Rate (kg/h)	800	900	1000	1100	1200	1500
	Temperature of Fuel Reactor (ºC)	950	950	950	950	950	950
	Temperature of Air Reactor (ºC)	935	935	935	935	935	935
	Fe_2O_3 flow in the Fuel Reactor (kg/h)	5921	5921	5921	5921	5921	5921
	Al_2O_3 in the System (kg/h)	3951	3951	3951	3951	3951	3951
	Particle Density (kg/m³)	3200	3200	3200	3200	3200	3200
Energy balance (kW)	Fuel Reactor	-161.8	-161.8	-161.8	-161.8	-161.8	-161.8
	Air Reactor	771.99	829.67	829.79	829.93	830.07	830.49
	Cool air reactor exhaust	151.97	173.08	197.33	221.58	245.83	318.57
	Cool flue gas	148.33	148.33	148.33	148.33	148.33	148.33
	Cool OC for air reactor	40.9	40.9	40.9	40.9	40.9	40.9
	Reheat OC for fuel reactor	-42.7	-42.7	-42.7	-42.7	-42.7	-42.7
	Heat steam	-69.8	-69.8	-69.8	-69.8	-68.8	-69.8
	Heat air	-206.6	-232.4	-258.2	-284.1	-309.9	-387.3
	Net	632.3	685.26	683.81	682.37	681.94	676.63

Table A.2 CLC process simulation results for different air flow rates with Colombian coal at 100 kg/h and Fe_2O_3/Al_2O_3 at 5000/3000 kg/h

Initial values	Coal (kg/h)	100	100	100	100	100	100
	Water (kg/h)	140	140	140	140	140	140
	Air Flow Rate (kg/h)	100	300	400	500	600	713
	Temperature of Fuel Reactor (ºC)	950	950	950	950	950	950
	Temperature of Air Reactor (ºC)	935	935	935	935	935	935
	Fe_2O_3 flow in the Fuel Reactor (kg/h)	5000	5000	5000	5000	5000	5000
	Al_2O_3 in the System (kg/h)	3000	3000	3000	3000	3000	3000
	Particle Density (kg/m³)	3200	3200	3200	3200	3200	3200
Energy balance (kW)	Fuel Reactor	-183.2	-183.2	-183.2	-183.2	-183.2	-183.2
	Air Reactor	96.498	289.5	386	482.49	578.99	688
	Cool air reactor exhaust	18.996	56.999	75.985	94.981	113.98	135.4
	Cool flue gas	142.63	142.63	142.63	142.63	142.63	142.63
	Cool OC for air reactor	32.792	32.792	32.792	32.792	32.792	32.792
	Reheat OC for fuel reactor	-34.27	-34.27	-34.27	-34.27	-34.27	-34.27
	Heat steam	-69.8	-69.8	-69.8	-69.8	-69.8	-69.8
	Heat air	-25.82	-77.47	-103.3	-129.1	-154.9	-184.1
	Net	-22.21	157.14	246.8	336.47	426.14	527.41
Initial values	Coal (kg/h)	100	100	100	100	100	100
	Water (kg/h)	140	140	140	140	140	140
	Air Flow Rate (kg/h)	800	900	1000	1100	1200	1500
	Temperature of Fuel Reactor (ºC)	950	950	950	950	950	950
	Temperature of Air Reactor (ºC)	935	935	935	935	935	935
	Fe_2O_3 flow in the Fuel Reactor (kg/h)	5000	5000	5000	5000	5000	5000
	Al_2O_3 in the System (kg/h)	3000	3000	3000	3000	3000	3000
	Particle Density (kg/m³)	3200	3200	3200	3200	3200	3200
Energy balance (kW)	Fuel Reactor	-183.2	-183.2	-183.2	-183.2	-183.2	-183.2
	Air Reactor	700.66	700.79	700.93	701.11	701.21	701.64
	Cool air reactor exhaust	155.86	180.1	204.35	228.6	252.85	325.59
	Cool flue gas	142.63	142.63	142.63	142.63	142.63	142.63
	Cool OC for air reactor	32.792	32.792	32.792	32.792	32.792	32.792
	Reheat OC for fuel reactor	-34.27	-34.27	-34.27	-34.27	-34.27	-34.27
	Heat steam	-69.8	-69.8	-69.8	-69.8	-69.8	-69.8
	Heat air	-206.6	-232.4	-258.2	-284.1	-309.9	-387.3
	Net	538.05	536.6	535.16	533.77	532.29	527.99

Table A.3 CLC process simulation results for different air flow rates with Colombian coal at 100 kg/h and Fe_2O_3/Al_2O_3 at 6500/4500 kg/h

Initial values	Coal (kg/h)	100	100	100	100	100	100
	Water (kg/h)	140	140	140	140	140	140
	Air Flow Rate (kg/h)	100	300	400	500	600	713
	Temperature of Fuel Reactor (ºC)	950	950	950	950	950	950
	Temperature of Air Reactor (ºC)	935	935	935	935	935	935
	Fe_2O_3 flow in the Fuel Reactor (kg/h)	6500	6500	6500	6500	6500	6500
	Al_2O_3 in the System (kg/h)	4500	4500	4500	4500	4500	4500
	Particle Density (kg/m³)	3200	3200	3200	3200	3200	3200
Energy balance (kW)	Fuel Reactor	-148.4	-148.4	-148.4	-148.4	-148.4	-148.4
	Air Reactor	96.498	289.5	386	482.49	578.99	688.04
	Cool air reactor exhaust	18.996	56.999	75.985	94.981	113.98	135.4
	Cool flue gas	151.96	151.96	151.96	151.96	151.96	151.96
	Cool OC for air reactor	45.781	45.781	45.781	45.781	45.781	45.781
	Reheat OC for fuel reactor	-47.71	-47.71	-47.71	-47.71	-47.71	-47.71
	Heat steam	-69.8	-69.8	-69.8	-69.8	-69.8	-69.8
	Heat air	-25.82	-77.47	-103.3	-129.1	-154.9	-184.1
	Net	21.473	200.83	290.49	380.16	469.83	571.14
Initial values	Coal (kg/h)	100	100	100	100	100	100
	Water (kg/h)	140	140	140	140	140	140
	Air Flow Rate (kg/h)	800	900	1000	1100	1200	1500
	Temperature of Fuel Reactor (ºC)	950	950	950	950	950	950
	Temperature of Air Reactor (ºC)	935	935	935	935	935	935
	Fe_2O_3 flow in the Fuel Reactor (kg/h)	6500	6500	6500	6500	6500	6500
	Al_2O_3 in the System (kg/h)	4500	4500	4500	4500	4500	4500
	Particle Density (kg/m³)	3200	3200	3200	3200	3200	3200
Energy balance (kW)	Fuel Reactor	-148.4	-148.4	-148.4	-148.4	-148.4	-148.4
	Air Reactor	771.99	868.49	910.81	910.94	911.07	911.49
	Cool air reactor exhaust	151.97	170.97	192.91	217.16	241.41	314.15
	Cool flue gas	151.96	151.96	151.96	151.96	151.96	151.96
	Cool OC for air reactor	45.781	45.781	45.781	45.781	45.781	45.781
	Reheat OC for fuel reactor	-47.71	-47.71	-47.71	-47.71	-47.71	-47.71
	Heat steam	-69.8	-69.8	-69.8	-69.8	-69.8	-69.8
	Heat air	-206.6	-232.4	-258.2	-284.1	-309.9	-387.3
	Net	649.18	738.85	777.29	775.85	774.41	770.1

Table A.4 CLC process simulation results for different air flow rates with Colombian coal at 100 kg/h and Fe_2O_3/Al_2O_3 at 7000/5000 kg/h

Initial values	Coal (kg/h)	100	100	100	100	100	100
	Water (kg/h)	140	140	140	140	140	140
	Air Flow Rate (kg/h)	100	300	400	500	600	713
	Temperature of Fuel Reactor (ºC)	950	950	950	950	950	950
	Temperature of Air Reactor (ºC)	935	935	935	935	935	935
	Fe_2O_3 flow in the Fuel Reactor (kg/h)	7000	7000	7000	7000	7000	7000
	Al_2O_3 in the System (kg/h)	5000	5000	5000	5000	5000	5000
	Particle Density (kg/m³)	3200	3200	3200	3200	3200	3200
Energy balance (kW)	Fuel Reactor	-139.6	-139.6	-139.6	-139.6	-139.6	-139.6
	Air Reactor	96.498	289.5	386	482.49	578.99	688.04
	Cool air reactor exhaust	18.996	56.999	75.985	94.981	113.98	135.4
	Cool flue gas	153.71	153.71	153.71	153.71	153.71	153.71
	Cool OC for air reactor	50.175	50.175	50.175	50.175	50.175	50.175
	Reheat OC for fuel reactor	-52.19	-52.19	-52.19	-52.19	-52.19	-52.19
	Heat steam	-69.8	-69.8	-69.8	-69.8	-69.8	-69.8
	Heat air	-25.82	-77.47	-103.3	-129.1	-154.9	-184.1
	Net	31.917	211.27	300.93	390.6	480.28	581.58
Initial values	Coal (kg/h)	100	100	100	100	100	100
	Water (kg/h)	140	140	140	140	140	140
	Air Flow Rate (kg/h)	800	900	1000	1100	1200	1500
	Temperature of Fuel Reactor (ºC)	950	950	950	950	950	950
	Temperature of Air Reactor (ºC)	935	935	935	935	935	935
	Fe_2O_3 flow in the Fuel Reactor (kg/h)	7000	7000	7000	7000	7000	7000
	Al_2O_3 in the System (kg/h)	5000	5000	5000	5000	5000	5000
	Particle Density (kg/m³)	3200	3200	3200	3200	3200	3200
Energy balance (kW)	Fuel Reactor	-139.6	-139.6	-139.6	-139.6	-139.6	-139.6
	Air Reactor	771.99	868.49	949.41	949.52	949.66	950.07
	Cool air reactor exhaust	151.97	170.97	190.81	215.06	239.31	312.05
	Cool flue gas	153.71	153.71	153.71	153.71	153.71	153.71
	Cool OC for air reactor	50.175	50.175	50.175	50.175	50.175	50.175
	Reheat OC for fuel reactor	-52.19	-52.19	-52.19	-52.19	-52.19	-52.19
	Heat steam	-69.8	-69.8	-69.8	-69.8	-68.8	-69.8
	Heat air	-206.6	-232.4	-258.2	-284.1	-309.9	-387.3
	Net	659.62	749.29	824.23	822.77	822.33	817.02

Table A.5 CLC process simulation results for different air flow rates with Colombian coal at 100 kg/h and Fe_2O_3/Al_2O_3 at 7500/5500 kg/h

Initial values	Coal (kg/h)	100	100	100	100	100	100
	Water (kg/h)	140	140	140	140	140	140
	Air Flow Rate (kg/h)	100	300	400	500	600	713
	Temperature of Fuel Reactor (ºC)	950	950	950	950	950	950
	Temperature of Air Reactor (ºC)	935	935	935	935	935	935
	Fe_2O_3 flow in the Fuel Reactor (kg/h)	7500	7500	7500	7500	7500	7500
	Al_2O_3 in the System (kg/h)	5500	5500	5500	5500	5500	5500
	Particle Density (kg/m³)	3200	3200	3200	3200	3200	3200
Energy balance (kW)	Fuel Reactor	-134.6	-134.6	-134.6	-134.6	-134.6	-134.6
	Air Reactor	96.498	289.5	386	482.49	578.99	688.04
	Cool air reactor exhaust	18.996	56.999	75.985	94.981	113.98	135.4
	Cool flue gas	153.71	153.71	153.71	153.71	153.71	153.71
	Cool OC for air reactor	54.647	54.647	54.647	54.647	54.647	54.647
	Reheat OC for fuel reactor	-56.67	-56.67	-56.67	-56.67	-56.67	-56.67
	Heat steam	-69.8	-69.8	-69.8	-69.8	-69.8	-69.8
	Heat air	-25.82	-77.47	-103.3	-129.1	-154.9	-184.1
	Net	36.942	216.3	305.96	395.63	485.3	586.61
Initial values	Coal (kg/h)	100	100	100	100	100	100
	Water (kg/h)	140	140	140	140	140	140
	Air Flow Rate (kg/h)	800	900	1000	1100	1200	1500
	Temperature of Fuel Reactor (ºC)	950	950	950	950	950	950
	Temperature of Air Reactor (ºC)	935	935	935	935	935	935
	Fe_2O_3 flow in the Fuel Reactor (kg/h)	7500	7500	7500	7500	7500	7500
	Al_2O_3 in the System (kg/h)	5500	5500	5500	5500	5500	5500
	Particle Density (kg/m³)	3200	3200	3200	3200	3200	3200
Energy balance (kW)	Fuel Reactor	-134.6	-134.6	-134.6	-134.6	-134.6	-134.6
	Air Reactor	771.99	868.49	949.41	949.52	949.66	950.07
	Cool air reactor exhaust	151.97	170.97	190.81	215.06	239.31	312.05
	Cool flue gas	153.71	153.71	153.71	153.71	153.71	153.71
	Cool OC for air reactor	54.647	54.647	54.647	54.647	54.647	54.647
	Reheat OC for fuel reactor	-56.67	-56.67	-56.67	-56.67	-56.67	-56.67
	Heat steam	-69.8	-69.8	-69.8	-69.8	-69.8	-69.8
	Heat air	-206.6	-232.4	-258.2	-284.1	-309.9	-387.3
	Net	664.65	754.32	829.25	827.8	826.35	822.04

Table A.6 CLC process simulation results for different air flow rates with Colombian coal at 100 kg/h and Fe_2O_3/Al_2O_3 at 8000/6000 kg/h

Initial values	Coal (kg/h)	100	100	100	100	100	100
	Water (kg/h)	140	140	140	140	140	140
	Air Flow Rate (kg/h)	100	300	400	500	600	713
	Temperature of Fuel Reactor (ºC)	950	950	950	950	950	950
	Temperature of Air Reactor (ºC)	935	935	935	935	935	935
	Fe_2O_3 flow in the Fuel Reactor (kg/h)	8000	8000	8000	8000	8000	8000
	Al_2O_3 in the System (kg/h)	6000	6000	6000	6000	6000	6000
	Particle Density (kg/m³)	3200	3200	3200	3200	3200	3200
Energy balance (kW)	Fuel Reactor	-129.6	-129.6	-129.6	-129.6	-129.6	-129.6
	Air Reactor	96.498	289.5	386	482.49	578.99	688.04
	Cool air reactor exhaust	18.996	56.999	75.985	94.981	113.98	135.4
	Cool flue gas	153.71	153.71	153.71	153.71	153.71	153.71
	Cool OC for air reactor	59.121	59.121	59.121	59.121	59.121	59.121
	Reheat OC for fuel reactor	-61.15	-61.15	-61.15	-61.15	-61.15	-61.15
	Heat steam	-69.8	-69.8	-69.8	-69.8	-69.8	-69.8
	Heat air	-25.82	-77.47	-103.3	-129.1	-154.9	-184.1
	Net	41.968	221.32	310.98	400.66	490.33	591.63
Initial values	Coal (kg/h)	100	100	100	100	100	100
	Water (kg/h)	140	140	140	140	140	140
	Air Flow Rate (kg/h)	800	900	1000	1100	1200	1500
	Temperature of Fuel Reactor (ºC)	950	950	950	950	950	950
	Temperature of Air Reactor (ºC)	935	935	935	935	935	935
	Fe_2O_3 flow in the Fuel Reactor (kg/h)	8000	8000	8000	8000	8000	8000
	Al_2O_3 in the System (kg/h)	6000	6000	6000	6000	6000	6000
	Particle Density (kg/m³)	3200	3200	3200	3200	3200	3200
Energy balance (kW)	Fuel Reactor	-129.6	-129.6	-129.6	-129.6	-129.6	-129.6
	Air Reactor	771.99	868.49	949.41	949.52	949.66	950.07
	Cool air reactor exhaust	151.97	170.97	190.81	215.06	239.31	312.05
	Cool flue gas	153.71	153.71	153.71	153.71	153.71	153.71
	Cool OC for air reactor	59.121	59.121	59.121	59.121	59.121	59.121
	Reheat OC for fuel reactor	-61.15	-61.15	-61.15	-61.15	-61.15	-61.15
	Heat steam	-69.8	-69.8	-69.8	-69.8	-68.8	-69.8
	Heat air	-206.6	-232.4	-258.2	-284.1	-309.9	-387.3
	Net	669.67	759.34	834.28	832.82	832.38	827.07

Table A.7 Scaled-up simulation results for different coal feeding rates using the baseline ratios of air flow rate and oxygen carrier feeding rate from the work of Sahir et al [1]

Initial values	Coal (kg/h)	100	500	1000	1500	2500
	Water (kg/h)	140	700	1400	2100	3500
	Air Flow Rate (kg/h)	713	3565	7130	10695	17825
	Temperature of Fuel Reactor (ºC)	950	950	950	950	950
	Temperature of Air Reactor (ºC)	935	935	935	935	935
	Fe_2O_3 flow in the Fuel Reactor (kg/h)	5921	30000	60000	90000	150000
	Al_2O_3 in the System (kg/h)	3951	20000	40000	60000	100000
	Particle Density (kg/m³)	3200	3200	3200	3200	3200
Energy balance (KW)	Fuel Reactor	-161.8	-800.8	-1602	-2402	-4.004
	Air Reactor	688	3440.2	6880.4	10321	17.201
	Cool air reactor exhaust	135.4	677.22	1354.4	2031.7	3.3861
	Cool flue gas	148.3	744.09	1488.2	2232.3	3.7205
	Cool OC for air reactor	40.9	207.26	414.52	621.77	1.0363
	Reheat OC for fuel reactor	-42.7	-216.2	-432.3	-648.5	-1.081
	Heat steam	-69.8	-349.1	-698.3	-1047	-1.746
	Heat air	-184.1	-920.6	-1841	-2762	-4.603
	Net	554.2	2782	5564.1	8346.1	13910
Initial values	Coal (kg/h)	3500	5000	8000	12000	
	Water (kg/h)	4900	7000	11200	16800	
	Air Flow Rate (kg/h)	24955	35650	57040	85560	
	Temperature of Fuel Reactor (ºC)	950	950	950	950	
	Temperature of Air Reactor (ºC)	935	935	935	935	
	Fe_2O_3 flow in the Fuel Reactor (kg/h)	210000	300000	480000	720000	
	Al_2O_3 in the System (kg/h)	140000	200000	320000	480000	
	Particle Density (kg/m³)	3200	3200	3200	3200	
Energy balance (KW)	Fuel Reactor	-5.606	-8.008	-12.81	-19.22	
	Air Reactor	24.081	34.402	55.043	82.564	
	Cool air reactor exhaust	4.7405	6.7722	10.836	16.253	
	Cool flue gas	5.2087	7.4409	11.906	17.858	
	Cool OC for air reactor	1.4508	2.0726	3.3161	4.9742	
	Reheat OC for fuel reactor	-1.513	-2.162	-3.459	-5.188	
	Heat steam	-2.444	-3.491	-5.586	-8.379	
	Heat air	-6.444	-9.206	-14.73	-22.09	
	Net	19474	27820	44513	66769	

Table A.8 Scaled-up simulation results for different coal feeding rates using the optimum ratios of air flow rate and oxygen carrier feeding rate

Initial values	Coal (kg/h)	100	500	1000	1500	2500
	Water (kg/h)	140	700	1400	2100	3500
	Air Flow Rate (kg/h)	1000	5000	10000	15000	25000
	Temperature of Fuel Reactor (ºC)	950	950	950	950	950
	Temperature of Air Reactor (ºC)	935	935	935	935	935
	Fe_2O_3 flow in the Fuel Reactor (kg/h)	7000	35000	70000	105000	175000
	Al_2O_3 in the System (kg/h)	5000	25000	50000	75000	125000
	Particle Density (kg/m³)	3200	3200	3200	3200	3200
Energy balance (KW)	Fuel Reactor	-139.6	-698.2	-1484	-2226	-3711
	Air Reactor	949.41	4747	9108.1	13662	22770
	Cool air reactor exhaust	190.81	954.06	1929.1	2893.7	4822.9
	Cool flue gas	153.71	768.54	1519.6	2279.4	3799
	Cool OC for air reactor	50.175	250.87	457.81	686.72	1144.5
	Reheat OC for fuel reactor	-52.19	-261	-477.1	-715.7	-1193
	Heat steam	-69.8	-349.1	-698.3	-1047	-1746
	Heat air	-258.2	-1291	-2582	-3873	-6456
	Net	824.23	4121	8242.3	12363	20606
Initial values	Coal (kg/h)	3500	5000	8000	12000	
	Water (kg/h)	4900	7000	11200	16800	
	Air Flow Rate (kg/h)	35000	50000	80000	120000	
	Temperature of Fuel Reactor (ºC)	950	950	950	950	
	Temperature of Air Reactor (ºC)	935	935	935	935	
	Fe_2O_3 flow in the Fuel Reactor (kg/h)	245000	350000	560000	840000	
	Al_2O_3 in the System (kg/h)	175000	250000	400000	600000	
	Particle Density (kg/m³)	3200	3200	3200	3200	
Energy balance (KW)	Fuel Reactor	-5195	-7421	-11874	-17811	
	Air Reactor	31878	45541	72865	109297	
	Cool air reactor exhaust	6752	9645.7	15433	23150	
	Cool flue gas	5318.6	7598.1	12157	18235	
	Cool OC for air reactor	1602.3	2289.1	3662.5	5493.7	
	Reheat OC for fuel reactor	-1670	-2386	-3817	-5725	
	Heat steam	-2444	-3491	-5586	-8379	
	Heat air	-9038	-12912	-20659	-30988	
	Net	28847	41211	65936	98907	

Table A.9 CLC process simulation results for different air flow rates with Colombian coal at 12000 kg/h and Fe_2O_3/Al_2O_3 at 780000/540000 kg/h

Initial values	Coal (kg/h)	12000	12000	12000	12000	12000	12000
	Water (kg/h)	16800	16800	16800	16800	16800	16800
	Air Flow Rate (kg/h)	12000	36000	48000	60000	72000	84000
	Temperature of Fuel Reactor (ºC)	950	950	950	950	950	950
	Temperature of Air Reactor (ºC)	935	935	935	935	935	935
	Fe_2O_3 flow in the Fuel Reactor (kg/h)	780000	780000	780000	780000	780000	780000
	Al_2O_3 in the System (kg/h)	540000	540000	540000	540000	540000	540000
	Particle Density (kg/m³)	3200	3200	3200	3200	3200	3200
Energy balance (KW)	Fuel Reactor	-17811	-17811	-17811	-17811	-17811	-17811
	Air Reactor	11580	34740	46320	57899	69479	81059
	Cool air reactor exhaust	2279.6	6838.7	9118.2	11398	13677	15957
	Cool flue gas	18235	18235	18235	18235	18235	18235
	Cool OC for air reactor	5493.7	5493.7	5493.7	5493.7	5493.7	5493.7
	Reheat OC for fuel reactor	-5725	-5725	-5725	-5725	-5725	-5725
	Heat steam	-8379	-8379	-8379	-8379	-8379	-8379
	Heat air	-3099	-9296	-12395	-15494	-18593	-21692
	Net	2573.3	24095	34855	45616	56376	67137
Initial values	Coal (kg/h)	12000	12000	12000	12000	12000	12000
	Water (kg/h)	16800	16800	16800	16800	16800	16800
	Air Flow Rate (kg/h)	96000	108000	120000	132000	144000	180000
	Temperature of Fuel Reactor (ºC)	950	950	950	950	950	950
	Temperature of Air Reactor (ºC)	935	935	935	935	935	935
	Fe_2O_3 flow in the Fuel Reactor (kg/h)	780000	780000	780000	780000	780000	780000
	Al_2O_3 in the System (kg/h)	540000	540000	540000	540000	540000	540000
	Particle Density (kg/m³)	3200	3200	3200	3200	3200	3200
Energy balance (KW)	Fuel Reactor	-17811	-17811	-17811	-17811	-17811	-17811
	Air Reactor	92639	104219	109297	109313	109329	109379
	Cool air reactor exhaust	18236	20516	23150	26059	28969	37698
	Cool flue gas	18235	18235	18235	18235	18235	18235
	Cool OC for air reactor	5493.7	5493.7	5493.7	5493.7	5493.7	5493.7
	Reheat OC for fuel reactor	-5725	-5725	-5725	-5725	-5725	-5725
	Heat steam	-8379	-8379	-8379	-8379	-8379	-8379
	Heat air	-24790	-27889	-30988	-34087	-37186	-46482
	Net	77898	88658	93271	93098	92925	92408

Table A.10 CLC process simulation results for different air flow rates with Colombian coal at 12000 kg/h and Fe_2O_3/Al_2O_3 at 840000/600000 kg/h

Initial values	Coal (kg/h)	12000	12000	12000	12000	12000	12000
	Water (kg/h)	16800	16800	16800	16800	16800	16800
	Air Flow Rate (kg/h)	12000	36000	48000	60000	72000	84000
	Temperature of Fuel Reactor (ºC)	950	950	950	950	950	950
	Temperature of Air Reactor (ºC)	935	935	935	935	935	935
	Fe_2O_3 flow in the Fuel Reactor (kg/h)	840000	840000	840000	840000	840000	840000
	Al_2O_3 in the System (kg/h)	600000	600000	600000	600000	600000	600000
	Particle Density (kg/m³)	3200	3200	3200	3200	3200	3200
Energy balance (KW)	Fuel Reactor	-16757	-16757	-16757	-16757	-16757	-16757
	Air Reactor	11580	34740	46320	57899	69479	81059
	Cool air reactor exhaust	2279.6	6838.7	9118.2	11398	13677	15957
	Cool flue gas	18445	18445	18445	18445	18445	18445
	Cool OC for air reactor	6021	6021	6021	6021	6021	6021
	Reheat OC for fuel reactor	-6263	-6263	-6263	-6263	-6263	-6263
	Heat steam	-8379	-8379	-8379	-8379	-8379	-8379
	Heat air	-3099	-9296	-12395	-15494	-18593	-21692
	Net	3826.8	25348	36109	46869	57630	68390
Initial values	Coal (kg/h)	12000	12000	12000	12000	12000	12000
	Water (kg/h)	16800	16800	16800	16800	16800	16800
	Air Flow Rate (kg/h)	96000	108000	120000	132000	144000	180000
	Temperature of Fuel Reactor (ºC)	950	950	950	950	950	950
	Temperature of Air Reactor (ºC)	935	935	935	935	935	935
	Fe_2O_3 flow in the Fuel Reactor (kg/h)	840000	840000	840000	840000	840000	840000
	Al_2O_3 in the System (kg/h)	600000	600000	600000	600000	600000	600000
	Particle Density (kg/m³)	3200	3200	3200	3200	3200	3200
Energy balance (KW)	Fuel Reactor	-16757	-16757	-16757	-16757	-16757	-16757
	Air Reactor	92639	104219	113929	113943	113959	114009
	Cool air reactor exhaust	18236	20516	22897	25807	28717	37446
	Cool flue gas	18445	18445	18445	18445	18445	18445
	Cool OC for air reactor	6021	6021	6021	6021	6021	6021
	Reheat OC for fuel reactor	-6263	-6263	-6263	-6263	-6263	-6263
	Heat steam	-8379	-8379	-8379	-8379	-8379	-8379
	Heat air	-24790	-27889	-30988	-34087	-37186	-46482
	Net	79151	89912	98904	98730	98556	98039

Table A.11 CLC process simulation results for different air flow rates with Colombian coal at 12000 kg/h and Fe_2O_3/Al_2O_3 at 900000/660000 kg/h

Initial values	Coal (kg/h)	12000	12000	12000	12000	12000	12000
	Water (kg/h)	16800	16800	16800	16800	16800	16800
	Air Flow Rate (kg/h)	12000	36000	48000	60000	72000	84000
	Temperature of Fuel Reactor (ºC)	950	950	950	950	950	950
	Temperature of Air Reactor (ºC)	935	935	935	935	935	935
	Fe_2O_3 flow in the Fuel Reactor (kg/h)	900000	900000	900000	900000	900000	900000
	Al_2O_3 in the System (kg/h)	660000	660000	660000	660000	660000	660000
	Particle Density (kg/m³)	3200	3200	3200	3200	3200	3200
Energy balance (KW)	Fuel Reactor	-16154	-16154	-16154	-16154	-16154	-16154
	Air Reactor	11580	34740	46320	57899	69479	81059
	Cool air reactor exhaust	2279.6	6838.7	9118.2	11398	13677	15957
	Cool flue gas	18445	18445	18445	18445	18445	18445
	Cool OC for air reactor	6557.7	6557.7	6557.7	6557.7	6557.7	6557.7
	Reheat OC for fuel reactor	-6801	-6801	-6801	-6801	-6801	-6801
	Heat steam	-8379	-8379	-8379	-8379	-8379	-8379
	Heat air	-3099	-9296	-12395	-15494	-18593	-21692
	Net	4429.8	25951	36712	47472	58233	68993
Initial values	Coal (kg/h)	12000	12000	12000	12000	12000	12000
	Water (kg/h)	16800	16800	16800	16800	16800	16800
	Air Flow Rate (kg/h)	96000	108000	120000	132000	144000	180000
	Temperature of Fuel Reactor (ºC)	950	950	950	950	950	950
	Temperature of Air Reactor (ºC)	935	935	935	935	935	935
	Fe_2O_3 flow in the Fuel Reactor (kg/h)	900000	900000	900000	900000	900000	900000
	Al_2O_3 in the System (kg/h)	660000	660000	660000	660000	660000	660000
	Particle Density (kg/m³)	3200	3200	3200	3200	3200	3200
Energy balance (KW)	Fuel Reactor	-16154	-16154	-16154	-16154	-16154	-16154
	Air Reactor	92639	104219	113929	113943	113959	114009
	Cool air reactor exhaust	18236	20516	22897	25807	28717	37446
	Cool flue gas	18445	18445	18445	18445	18445	18445
	Cool OC for air reactor	6557.7	6557.7	6557.7	6557.7	6557.7	6557.7
	Reheat OC for fuel reactor	-6801	-6801	-6801	-6801	-6801	-6801
	Heat steam	-8379	-8379	-8379	-8379	-8379	-8379
	Heat air	-24790	-27889	-30988	-34087	-37186	-46482
	Net	79754	90515	99507	99333	99159	98642

Table A.12 CLC process simulation results for different air flow rates with Bituminous coal at 100 kg/h and Fe_2O_3/Al_2O_3 at 5921/3951 kg/h

Initial values	Coal (kg/h)	100	100	100	100	100	100
	Water (kg/h)	140	140	140	140	140	140
	Air Flow Rate (kg/h)	100	300	400	500	600	713
	Temperature of Fuel Reactor (ºC)	950	950	950	950	950	950
	Temperature of Air Reactor (ºC)	935	935	935	935	935	935
	Fe_2O_3 flow in the Fuel Reactor (kg/h)	5921	5921	5921	5921	5921	5921
	Al_2O_3 in the System (kg/h)	3951	3951	3951	3951	3951	3951
	Particle Density (kg/m³)	3200	3200	3200	3200	3200	3200
Energy balance (kW)	Fuel Reactor	72.119	72.119	72.119	72.119	72.119	72.119
	Air Reactor	96.498	289.497	385.995	482.494	578.993	688
	Cool air reactor exhaust	18.996	56.988	75.985	94.981	113.978	135.4
	Cool flue gas	137.064	137.064	137.064	137.064	137.064	137.064
	Cool OC for air reactor	41.082	41.082	41.082	41.082	41.082	41.082
	Reheat OC for fuel reactor	-42.7	-42.7	-42.7	-42.7	-42.7	-42.7
	Heat steam	-69.8	-69.8	-69.8	-69.8	-69.8	-69.8
	Heat air	-25.823	-77.469	-103.29	-129.12	-154.94	-184.1
	Net	227.436	406.781	496.452	586.124	675.796	777.065
Initial values	Coal (kg/h)	100	100	100	100	100	100
	Water (kg/h)	140	140	140	140	140	140
	Air Flow Rate (kg/h)	800	900	1000	1100	1200	1500
	Temperature of Fuel Reactor (ºC)	950	950	950	950	950	950
	Temperature of Air Reactor (ºC)	935	935	935	935	935	935
	Fe_2O_3 flow in the Fuel Reactor (kg/h)	5921	5921	5921	5921	5921	5921
	Al_2O_3 in the System (kg/h)	3951	3951	3951	3951	3951	3951
	Particle Density (kg/m³)	3200	3200	3200	3200	3200	3200
Energy balance (kW)	Fuel Reactor	72.119	72.119	72.119	72.119	72.119	72.119
	Air Reactor	752.554	752.667	752.812	752.951	753.091	753.515
	Cool air reactor exhaust	153.029	177.277	201.524	225.772	250.02	322.764
	Cool flue gas	137.064	137.064	137.064	137.064	137.064	137.064
	Cool OC for air reactor	41.082	41.082	41.082	41.082	41.082	41.082
	Reheat OC for fuel reactor	-42.7	-42.7	-42.7	-42.7	-42.7	-42.7
	Heat steam	-69.8	-69.8	-69.8	-69.8	-69.8	-69.8
	Heat air	-206.59	-232.41	-258.23	-284.06	-309.88	-387.35
	Net	836.762	835.299	833.868	832.432	830.996	826.695

Table A.13 CLC process simulation results for different air flow rates with Anthracite coal at 100 kg/h and Fe_2O_3/Al_2O_3 at 5921/3951 kg/h

Initial values	Coal (kg/h)	100	100	100	100	100	100
	Water (kg/h)	140	140	140	140	140	140
	Air Flow Rate (kg/h)	100	300	400	500	600	713
	Temperature of Fuel Reactor (ºC)	950	950	950	950	950	950
	Temperature of Air Reactor (ºC)	935	935	935	935	935	935
	Fe_2O_3 flow in the Fuel Reactor (kg/h)	5921	5921	5921	5921	5921	5921
	Al_2O_3 in the System (kg/h)	3951	3951	3951	3951	3951	3951
	Particle Density (kg/m³)	3200	3200	3200	3200	3200	3200
Energy balance (kW)	Fuel Reactor	116.145	116.145	116.145	116.145	116.145	116.145
	Air Reactor	96.498	289.497	385.995	482.494	578.993	688
	Cool air reactor exhaust	18.996	56.988	75.985	94.981	113.978	135.4
	Cool flue gas	127.834	127.834	127.834	127.834	127.834	127.834
	Cool OC for air reactor	41.132	41.132	41.132	41.132	41.132	41.132
	Reheat OC for fuel reactor	-42.7	-42.7	-42.7	-42.7	-42.7	-42.7
	Heat steam	-69.8	-69.8	-69.8	-69.8	-69.8	-69.8
	Heat air	-25.823	-77.469	-103.29	-129.11	-154.94	-184.1
	Net	262.282	441.627	531.298	620.97	710.642	811.911
Initial values	Coal (kg/h)	100	100	100	100	100	100
	Water (kg/h)	140	140	140	140	140	140
	Air Flow Rate (kg/h)	800	900	1000	1100	1200	1500
	Temperature of Fuel Reactor (ºC)	950	950	950	950	950	950
	Temperature of Air Reactor (ºC)	935	935	935	935	935	935
	Fe_2O_3 flow in the Fuel Reactor (kg/h)	5921	5921	5921	5921	5921	5921
	Al_2O_3 in the System (kg/h)	3951	3951	3951	3951	3951	3951
	Particle Density (kg/m³)	3200	3200	3200	3200	3200	3200
Energy balance (kW)	Fuel Reactor	116.145	116.145	116.145	116.145	116.145	116.145
	Air Reactor	728.287	728.416	728.553	728.692	728.832	729.257
	Cool air reactor exhaust	154.351	178.599	202.847	227.094	251.342	324.086
	Cool flue gas	127.834	127.834	127.834	127.834	127.834	127.834
	Cool OC for air reactor	41.132	41.132	41.132	41.132	41.132	41.132
	Reheat OC for fuel reactor	-42.7	-42.7	-42.7	-42.7	-42.7	-42.7
	Heat steam	-69.8	-69.8	-69.8	-69.8	-69.8	-69.8
	Heat air	-206.58	-232.41	-258.23	-284.05	-309.88	-387.34
	Net	848.663	847.216	845.778	844.341	842.905	838.605

Table A.14 CLC process simulation results for different air flow rates with Lignite coal at 100 kg/h and Fe_2O_3/Al_2O_3 at 5921/3951 kg/h

Initial values	Coal (kg/h)	100	100	100	100	100	100
	Water (kg/h)	140	140	140	140	140	140
	Air Flow Rate (kg/h)	100	300	400	500	600	713
	Temperature of Fuel Reactor (ºC)	950	950	950	950	950	950
	Temperature of Air Reactor (ºC)	935	935	935	935	935	935
	Fe_2O_3 flow in the Fuel Reactor (kg/h)	5921	5921	5921	5921	5921	5921
	Al_2O_3 in the System (kg/h)	3951	3951	3951	3951	3951	3951
	Particle Density (kg/m³)	3200	3200	3200	3200	3200	3200
Energy balance (kW)	Fuel Reactor	246.014	246.014	246.014	246.014	246.014	246.014
	Air Reactor	96.498	289.497	385.995	475.591	475.716	475.872
	Cool air reactor exhaust	18.996	56.988	75.985	95.357	119.605	147.005
	Cool flue gas	115.4	115.4	115.4	115.4	115.4	115.4
	Cool OC for air reactor	41.649	41.649	41.649	41.649	41.649	41.649
	Reheat OC for fuel reactor	-42.7	-42.7	-42.7	-42.7	-42.7	-42.7
	Heat steam	-69.8	-69.8	-69.8	-69.8	-69.8	-69.8
	Heat air	-25.823	-77.46	-103.29	-129.11	-154.94	-184.1
	Net	380.234	559.579	649.25	732.395	730.944	729.34
Initial values	Coal (kg/h)	100	100	100	100	100	100
	Water (kg/h)	140	140	140	140	140	140
	Air Flow Rate (kg/h)	800	900	1000	1100	1200	1500
	Temperature of Fuel Reactor (ºC)	950	950	950	950	950	950
	Temperature of Air Reactor (ºC)	935	935	935	935	935	935
	Fe_2O_3 flow in the Fuel Reactor (kg/h)	5921	5921	5921	5921	5921	5921
	Al_2O_3 in the System (kg/h)	3951	3951	3951	3951	3951	3951
	Particle Density (kg/m³)	3200	3200	3200	3200	3200	3200
Energy balance (kW)	Fuel Reactor	246.014	246.014	246.014	246.014	246.014	246.014
	Air Reactor	475.994	476.136	476.278	476.42	476.563	476.992
	Cool air reactor exhaust	168.101	192.349	216.596	240.884	265.092	337.836
	Cool flue gas	115.4	115.4	115.4	115.4	115.4	115.4
	Cool OC for air reactor	41.649	41.649	41.649	41.649	41.649	41.649
	Reheat OC for fuel reactor	-42.7	-42.7	-42.7	-42.7	-42.7	-42.7
	Heat steam	-69.8	-69.8	-69.8	-69.8	-69.8	-69.8
	Heat air	-206.58	-232.41	-258.23	-284.05	-309.88	-387.34
	Net	728.072	726.638	725.204	723.811	722.338	718.042

Table A.15 CLC process simulation results for different air flow rates with Bituminous coal at 100 kg/h and Fe_2O_3/Al_2O_3 at 5000/3000 kg/h

Initial values	Coal (kg/h)	100	100	100	100	100	100
	Water (kg/h)	140	140	140	140	140	140
	Air Flow Rate (kg/h)	100	300	400	500	600	713
	Temperature of Fuel Reactor (ºC)	950	950	950	950	950	950
	Temperature of Air Reactor (ºC)	935	935	935	935	935	935
	Fe_2O_3 flow in the Fuel Reactor (kg/h)	5000	5000	5000	5000	5000	5000
	Al_2O_3 in the System (kg/h)	3000	3000	3000	3000	3000	3000
	Particle Density (kg/m³)	3200	3200	3200	3200	3200	3200
Energy balance (kW)	Fuel Reactor	57.719	57.719	57.719	57.719	57.719	57.719
	Air Reactor	96.498	289.497	385.995	482.494	578.993	688
	Cool air reactor exhaust	18.996	56.988	75.985	94.981	113.978	135.4
	Cool flue gas	134.734	134.734	134.734	134.734	134.734	134.734
	Cool OC for air reactor	32.792	32.792	32.792	32.792	32.792	32.792
	Reheat OC for fuel reactor	-34.273	-34.273	-34.273	-34.273	-34.273	-34.273
	Heat steam	-69.8	-69.8	-69.8	-69.8	-69.8	-69.8
	Heat air	-25.82	-77.46	-103.29	-129.11	-154.94	-184.1
	Net	210.843	390.188	479.859	569.531	659.203	760.472
Initial values	Coal (kg/h)	100	100	100	100	100	100
	Water (kg/h)	140	140	140	140	140	140
	Air Flow Rate (kg/h)	800	900	1000	1100	1200	1500
	Temperature of Fuel Reactor (ºC)	950	950	950	950	950	950
	Temperature of Air Reactor (ºC)	935	935	935	935	935	935
	Fe_2O_3 flow in the Fuel Reactor (kg/h)	5000	5000	5000	5000	5000	5000
	Al_2O_3 in the System (kg/h)	3000	3000	3000	3000	3000	3000
	Particle Density (kg/m³)	3200	3200	3200	3200	3200	3200
Energy balance (kW)	Fuel Reactor	57.719	57.719	57.719	57.719	57.719	57.719
	Air Reactor	700.662	700.794	700.932	701.072	701.213	701.639
	Cool air reactor exhaust	155.856	180.104	204.352	228.6	252.848	325.591
	Cool flue gas	134.734	134.734	134.734	134.734	134.734	134.734
	Cool OC for air reactor	32.792	32.792	32.792	32.792	32.792	32.792
	Reheat OC for fuel reactor	-34.273	-34.273	-34.273	-34.273	-34.273	-34.273
	Heat steam	-69.8	-69.8	-69.8	-69.8	-69.8	-69.8
	Heat air	-206.58	-232.41	-258.23	-284.05	-309.88	-387.34
	Net	771.104	769.66	768.223	766.788	765.353	761.053

Table A.16 CLC process simulation results for different air flow rates with Bituminous coal at 100 kg/h and Fe_2O_3/Al_2O_3 at 5500/3500 kg/h

Initial values	Coal (kg/h)	100	100	100	100	100	100
	Water (kg/h)	140	140	140	140	140	140
	Air Flow Rate (kg/h)	100	300	400	500	600	713
	Temperature of Fuel Reactor (ºC)	950	950	950	950	950	950
	Temperature of Air Reactor (ºC)	935	935	935	935	935	935
	Fe_2O_3 flow in the Fuel Reactor (kg/h)	5500	5500	5500	5500	5500	5500
	Al_2O_3 in the System (kg/h)	3500	3500	3500	3500	3500	3500
	Particle Density (kg/m³)	3200	3200	3200	3200	3200	3200
Energy balance (kW)	Fuel Reactor	67.705	67.705	67.705	67.705	67.705	67.705
	Air Reactor	96.498	289.497	385.995	482.494	578.993	688.037
	Cool air reactor exhaust	18.9963	56.9989	75.985	94.981	113.978	135.4
	Cool flue gas	137.064	137.064	137.064	137.064	137.064	137.064
	Cool OC for air reactor	37.159	37.159	37.159	37.159	37.159	37.159
	Reheat OC for fuel reactor	-38.752	-38.752	-38.752	-38.752	-38.752	-38.752
	Heat steam	-69.8	-69.8	-69.8	-69.8	-69.8	-69.8
	Heat air	-25.82	-77.46	-103.29	-129.11	-154.94	-184.12
	Net	223.047	402.4029	492.063	581.735	671.407	772.693
Initial values	Coal (kg/h)	100	100	100	100	100	100
	Water (kg/h)	140	140	140	140	140	140
	Air Flow Rate (kg/h)	800	900	1000	1100	1200	1500
	Temperature of Fuel Reactor (ºC)	950	950	950	950	950	950
	Temperature of Air Reactor (ºC)	935	935	935	935	935	935
	Fe_2O_3 flow in the Fuel Reactor (kg/h)	5500	5500	5500	5500	5500	5500
	Al_2O_3 in the System (kg/h)	3500	3500	3500	3500	3500	3500
	Particle Density (kg/m³)	3200	3200	3200	3200	3200	3200
Energy balance (kW)	Fuel Reactor	67.705	67.705	67.705	67.705	67.705	67.705
	Air Reactor	752.554	752.677	752.812	752.951	753.091	753.515
	Cool air reactor exhaust	153.029	177.277	201.524	225.773	250.02	322.764
	Cool flue gas	137.064	137.064	137.064	137.064	137.064	137.064
	Cool OC for air reactor	37.159	37.159	37.159	37.159	37.159	37.159
	Reheat OC for fuel reactor	-38.752	-38.752	-38.752	-38.752	-38.752	-38.752
	Heat steam	-69.8	-69.8	-69.8	-69.8	-69.8	-69.8
	Heat air	-206.58	-232.41	-258.23	-284.05	-309.88	-387.34
	Net	832.373	830.92	829.479	828.044	826.607	822.306

Table A.17 CLC process simulation results for different air flow rates with Bituminous coal at 100 kg/h and Fe_2O_3/Al_2O_3 at 7000/5000 kg/h

Initial values	Coal (kg/h)	100	100	100	100	100	100
	Water (kg/h)	140	140	140	140	140	140
	Air Flow Rate (kg/h)	100	300	400	500	600	713
	Temperature of Fuel Reactor (ºC)	950	950	950	950	950	950
	Temperature of Air Reactor (ºC)	935	935	935	935	935	935
	Fe_2O_3 flow in the Fuel Reactor (kg/h)	7000	7000	7000	7000	7000	7000
	Al_2O_3 in the System (kg/h)	5000	5000	5000	5000	5000	5000
	Particle Density (kg/m³)	3200	3200	3200	3200	3200	3200
Energy balance (kW)	Fuel Reactor	82.8	82.8	82.8	82.8	82.8	82.8
	Air Reactor	96.49	289.497	385.995	482.494	578.993	688.037
	Cool air reactor exhaust	18.99	56.9989	75.985	94.981	113.978	135.4
	Cool flue gas	137.06	137.064	137.064	137.064	137.064	137.064
	Cool OC for air reactor	50.57	50.577	50.577	50.577	50.577	50.577
	Reheat OC for fuel reactor	-52.19	-52.192	-52.192	-52.192	-52.192	-52.192
	Heat steam	-69.80	-69.8	-69.8	-69.8	-69.8	-69.8
	Heat air	-25.82	-77.46	-103.29	-129.11	-154.94	-184.12
	Net	238.12	417.4759	507.136	596.808	686.48	787.766
Initial values	Coal (kg/h)	100	100	100	100	100	100
	Water (kg/h)	140	140	140	140	140	140
	Air Flow Rate (kg/h)	800	900	1000	1100	1200	1500
	Temperature of Fuel Reactor (ºC)	950	950	950	950	950	950
	Temperature of Air Reactor (ºC)	935	935	935	935	935	935
	Fe_2O_3 flow in the Fuel Reactor (kg/h)	7000	7000	7000	7000	7000	7000
	Al_2O_3 in the System (kg/h)	5000	5000	5000	5000	5000	5000
	Particle Density (kg/m³)	3200	3200	3200	3200	3200	3200
Energy balance (kW)	Fuel Reactor	82.8	82.8	82.8	82.8	82.8	82.8
	Air Reactor	752.554	752.677	752.812	752.951	753.091	753.515
	Cool air reactor exhaust	153.029	177.277	201.524	225.772	250.02	322.764
	Cool flue gas	137.064	137.064	137.064	137.064	137.064	137.064
	Cool OC for air reactor	50.577	50.577	50.577	50.577	50.577	50.577
	Reheat OC for fuel reactor	-52.192	-52.192	-52.192	-52.192	-52.192	-52.192
	Heat steam	-69.8	-69.8	-69.8	-69.8	-69.8	-69.8
	Heat air	-206.58	-232.41	-258.23	-284.05	-309.88	-387.34
	Net	847.446	845.993	844.552	843.116	841.68	837.379

Table A. 18 CLC process simulation results for different air flow rates with Anthracite coal at 100 kg/h and Fe_2O_3/Al_2O_3 at 5000/3000 kg/h

Initial values	Coal (kg/h)	100	100	100	100	100	100
	Water (kg/h)	140	140	140	140	140	140
	Air Flow Rate (kg/h)	100	300	400	500	600	713
	Temperature of Fuel Reactor (ºC)	950	950	950	950	950	950
	Temperature of Air Reactor (ºC)	935	935	935	935	935	935
	Fe_2O_3 flow in the Fuel Reactor (kg/h)	5000	5000	5000	5000	5000	5000
	Al_2O_3 in the System (kg/h)	3000	3000	3000	3000	3000	3000
	Particle Density (kg/m³)	3200	3200	3200	3200	3200	3200
Energy balance (kW)	Fuel Reactor	104.05	104.05	104.05	104.05	104.05	104.05
	Air Reactor	96.50	289.50	386.00	482.49	578.99	688.04
	Cool air reactor exhaust	19.00	56.99	75.99	94.98	113.98	135.44
	Cool flue gas	126.59	126.59	126.59	126.59	126.59	126.59
	Cool OC for air reactor	32.79	32.79	32.79	32.79	32.79	32.79
	Reheat OC for fuel reactor	-34.27	-34.27	-34.27	-34.27	-34.27	-34.27
	Heat steam	-69.80	-69.80	-69.80	-69.80	-69.80	-69.80
	Heat air	-25.82	-77.47	-103.29	-129.12	-154.94	-184.12
	Net	249.03	428.37	518.05	607.72	697.39	798.72
Initial values	Coal (kg/h)	100	100	100	100	100	100
	Water (kg/h)	140	140	140	140	140	140
	Air Flow Rate (kg/h)	800	900	1000	1100	1200	1500
	Temperature of Fuel Reactor (ºC)	950	950	950	950	950	950
	Temperature of Air Reactor (ºC)	935	935	935	935	935	935
	Fe_2O_3 flow in the Fuel Reactor (kg/h)	5000	5000	5000	5000	5000	5000
	Al_2O_3 in the System (kg/h)	3000	3000	3000	3000	3000	3000
	Particle Density (kg/m³)	3200	3200	3200	3200	3200	3200
Energy balance (kW)	Fuel Reactor	104.05	104.05	104.05	104.05	104.05	104.05
	Air Reactor	700.66	700.79	700.93	701.07	701.21	701.64
	Cool air reactor exhaust	155.86	180.10	204.35	228.60	252.85	325.59
	Cool flue gas	126.59	126.59	126.59	126.59	126.59	126.59
	Cool OC for air reactor	32.79	32.79	32.79	32.79	32.79	32.79
	Reheat OC for fuel reactor	-34.27	-34.27	-34.27	-34.27	-34.27	-34.27
	Heat steam	-69.80	-69.80	-69.80	-69.80	-69.80	-69.80
	Heat air	-206.59	-232.41	-258.23	-284.06	-309.88	-387.35
	Net	809.29	807.85	806.41	804.97	803.54	799.24

Table A.19 process simulation results for different air flow rates with Anthracite coal at 100 kg/h and Fe_2O_3/Al_2O_3 at 5200/3200 kg/h

Initial values	Coal (kg/h)	100	100	100	100	100	100
	Water (kg/h)	140	140	140	140	140	140
	Air Flow Rate (kg/h)	100	300	400	500	600	713
	Temperature of Fuel Reactor (ºC)	950	950	950	950	950	950
	Temperature of Air Reactor (ºC)	935	935	935	935	935	935
	Fe_2O_3 flow in the Fuel Reactor (kg/h)	5200	5200	5200	5200	5200	5200
	Al_2O_3 in the System (kg/h)	3200	3200	3200	3200	3200	3200
	Particle Density (kg/m³)	3200	3200	3200	3200	3200	3200
Energy balance (kW)	Fuel Reactor	108.71	108.71	108.71	108.71	108.71	108.71
	Air Reactor	96.50	289.50	386.00	482.49	578.99	688.04
	Cool air reactor exhaust	19.00	56.99	75.99	94.98	113.98	135.44
	Cool flue gas	127.83	127.83	127.83	127.83	127.83	127.83
	Cool OC for air reactor	34.53	34.53	34.53	34.53	34.53	34.53
	Reheat OC for fuel reactor	-36.07	-36.07	-36.07	-36.07	-36.07	-36.07
	Heat steam	-69.80	-69.80	-69.80	-69.80	-69.80	-69.80
	Heat air	-25.82	-77.47	-103.29	-129.12	-154.94	-184.12
	Net	254.88	434.22	523.89	613.57	703.24	804.57
Initial values	Coal (kg/h)	100	100	100	100	100	100
	Water (kg/h)	140	140	140	140	140	140
	Air Flow Rate (kg/h)	800	900	1000	1100	1200	1500
	Temperature of Fuel Reactor (ºC)	950	950	950	950	950	950
	Temperature of Air Reactor (ºC)	935	935	935	935	935	935
	Fe_2O_3 flow in the Fuel Reactor (kg/h)	5200	5200	5200	5200	5200	5200
	Al_2O_3 in the System (kg/h)	3200	3200	3200	3200	3200	3200
	Particle Density (kg/m³)	3200	3200	3200	3200	3200	3200
Energy balance (kW)	Fuel Reactor	108.71	108.71	108.71	108.71	108.71	108.71
	Air Reactor	728.29	728.42	728.55	728.69	728.83	729.26
	Cool air reactor exhaust	154.35	178.60	202.85	227.09	251.34	324.09
	Cool flue gas	127.83	127.83	127.83	127.83	127.83	127.83
	Cool OC for air reactor	34.53	34.53	34.53	34.53	34.53	34.53
	Reheat OC for fuel reactor	-36.07	-36.07	-36.07	-36.07	-36.07	-36.07
	Heat steam	-69.80	-69.80	-69.80	-69.80	-69.80	-69.80
	Heat air	-206.59	-232.41	-258.23	-284.06	-309.88	-387.35
	Net	841.26	839.81	838.37	836.94	835.50	831.20

Table A.20 CLC process simulation results for different air flow rates with Anthracite coal at 100 kg/h and Fe_2O_3/Al_2O_3 at 5500/3500 kg/h

Initial values	Coal (kg/h)	100	100	100	100	100	100
	Water (kg/h)	140	140	140	140	140	140
	Air Flow Rate (kg/h)	100	300	400	500	600	713
	Temperature of Fuel Reactor (ºC)	950	950	950	950	950	950
	Temperature of Air Reactor (ºC)	935	935	935	935	935	935
	Fe_2O_3 flow in the Fuel Reactor (kg/h)	5500	5500	5500	5500	5500	5500
	Al_2O_3 in the System (kg/h)	3500	3500	3500	3500	3500	3500
	Particle Density (kg/m³)	3200	3200	3200	3200	3200	3200
Energy balance (kW)	Fuel Reactor	111.73	111.73	111.73	111.73	111.73	111.73
	Air Reactor	96.50	289.50	386.00	482.49	578.99	688.04
	Cool air reactor exhaust	19.00	56.99	75.99	94.98	113.98	135.40
	Cool flue gas	127.83	127.83	127.83	127.83	127.83	127.83
	Cool OC for air reactor	37.03	37.03	37.03	37.03	37.03	37.03
	Reheat OC for fuel reactor	-38.75	-38.75	-38.75	-38.75	-38.75	-38.75
	Heat steam	-69.80	-69.80	-69.80	-69.80	-69.80	-69.80
	Heat air	-25.82	-77.47	-103.29	-129.12	-154.94	-184.12
	Net	257.71	437.06	526.73	616.40	706.07	807.36
Initial values	Coal (kg/h)	100	100	100	100	100	100
	Water (kg/h)	140	140	140	140	140	140
	Air Flow Rate (kg/h)	800	900	1000	1100	1200	1500
	Temperature of Fuel Reactor (ºC)	950	950	950	950	950	950
	Temperature of Air Reactor (ºC)	935	935	935	935	935	935
	Fe_2O_3 flow in the Fuel Reactor (kg/h)	5500	5500	5500	5500	5500	5500
	Al_2O_3 in the System (kg/h)	3500	3500	3500	3500	3500	3500
	Particle Density (kg/m³)	3200	3200	3200	3200	3200	3200
Energy balance (kW)	Fuel Reactor	111.73	111.73	111.73	111.73	111.73	111.73
	Air Reactor	728.29	728.42	728.55	728.69	728.83	729.26
	Cool air reactor exhaust	154.35	178.60	202.85	227.09	251.34	324.09
	Cool flue gas	127.83	127.83	127.83	127.83	127.83	127.83
	Cool OC for air reactor	37.03	37.03	37.03	37.03	37.03	37.03
	Reheat OC for fuel reactor	-38.75	-38.75	-38.75	-38.75	-38.75	-38.75
	Heat steam	-69.80	-69.80	-69.80	-69.80	-69.80	-69.80
	Heat air	-206.59	-232.41	-258.23	-284.06	-309.88	-387.35
	Net	844.09	842.65	841.21	839.77	838.34	834.04

Table A.21 CLC process simulation results for different air flow rates with Lignite coal at 100 kg/h and Fe_2O_3/Al_2O_3 at 3000/1000 kg/h

Initial values	Coal (kg/h)	100	100	100	100	100	100
	Water (kg/h)	140	140	140	140	140	140
	Air Flow Rate (kg/h)	100	300	400	500	600	713
	Temperature of Fuel Reactor (ºC)	950	950	950	950	950	950
	Temperature of Air Reactor (ºC)	935	935	935	935	935	935
	Fe_2O_3 flow in the Fuel Reactor (kg/h)	3000	3000	3000	3000	3000	3000
	Al_2O_3 in the System (kg/h)	1000	1000	1000	1000	1000	1000
	Particle Density (kg/m³)	3200	3200	3200	3200	3200	3200
Energy balance (kW)	Fuel Reactor	212.04	212.04	212.04	212.04	212.04	212.04
	Air Reactor	96.50	289.50	386.00	420.42	420.60	420.72
	Cool air reactor exhaust	19.00	56.99	75.99	98.36	122.61	150.01
	Cool flue gas	113.10	113.10	113.10	113.10	113.10	113.10
	Cool OC for air reactor	15.47	15.47	15.47	15.47	15.47	15.47
	Reheat OC for fuel reactor	-16.35	-16.35	-16.35	-16.35	-16.35	-16.35
	Heat steam	-69.80	-69.80	-69.80	-69.80	-69.80	-69.80
	Heat air	-25.82	-77.47	-103.29	-129.12	-154.94	-184.10
	Net	344.13	523.48	613.15	644.13	642.73	641.09
Initial values	Coal (kg/h)	100	100	100	100	100	100
	Water (kg/h)	140	140	140	140	140	140
	Air Flow Rate (kg/h)	800	900	1000	1100	1200	1500
	Temperature of Fuel Reactor (ºC)	950	950	950	950	950	950
	Temperature of Air Reactor (ºC)	935	935	935	935	935	935
	Fe_2O_3 flow in the Fuel Reactor (kg/h)	3000	3000	3000	3000	3000	3000
	Al_2O_3 in the System (kg/h)	1000	1000	1000	1000	1000	1000
	Particle Density (kg/m³)	3200	3200	3200	3200	3200	3200
Energy balance (kW)	Fuel Reactor	212.04	212.04	212.04	212.04	212.04	212.04
	Air Reactor	420.84	420.98	421.13	421.27	421.41	421.84
	Cool air reactor exhaust	171.11	195.36	219.60	243.85	268.10	340.84
	Cool flue gas	113.10	113.10	113.10	113.10	113.10	113.10
	Cool OC for air reactor	15.47	15.47	15.47	15.47	15.47	15.47
	Reheat OC for fuel reactor	-16.35	-16.35	-16.35	-16.35	-16.35	-16.35
	Heat steam	-69.80	-69.80	-69.80	-69.80	-69.80	-69.80
	Heat air	-206.59	-232.41	-258.23	-284.06	-309.88	-387.35
	Net	639.82	638.39	636.96	635.52	634.09	629.79

Table A.22 CLC process simulation results for different air flow rates with Lignite coal at 100 kg/h and Fe_2O_3/Al_2O_3 at 3500/1500 kg/h

Initial values	Coal (kg/h)	100	100	100	100	100	100
	Water (kg/h)	140	140	140	140	140	140
	Air Flow Rate (kg/h)	100	300	400	500	600	713
	Temperature of Fuel Reactor (ºC)	950	950	950	950	950	950
	Temperature of Air Reactor (ºC)	935	935	935	935	935	935
	Fe_2O_3 flow in the Fuel Reactor (kg/h)	3500	3500	3500	3500	3500	3500
	Al_2O_3 in the System (kg/h)	1500	1500	1500	1500	1500	1500
	Particle Density (kg/m³)	3200	3200	3200	3200	3200	3200
Energy balance (kW)	Fuel Reactor	221.47	221.47	221.47	221.47	221.47	221.47
	Air Reactor	96.50	289.50	386.00	475.59	475.72	475.87
	Cool air reactor exhaust	19.00	56.99	75.99	95.36	119.61	147.01
	Cool flue gas	115.40	115.40	115.40	115.40	115.40	115.40
	Cool OC for air reactor	19.83	19.83	19.83	19.83	19.83	19.83
	Reheat OC for fuel reactor	-20.83	-20.83	-20.83	-20.83	-20.83	-20.83
	Heat steam	-69.80	-69.80	-69.80	-69.80	-69.80	-69.80
	Heat air	-25.82	-77.47	-103.29	-129.12	-154.94	-184.10
	Net	355.74	535.09	624.76	707.91	706.45	704.85
Initial values	Coal (kg/h)	100	100	100	100	100	100
	Water (kg/h)	140	140	140	140	140	140
	Air Flow Rate (kg/h)	800	900	1000	1100	1200	1500
	Temperature of Fuel Reactor (ºC)	950	950	950	950	950	950
	Temperature of Air Reactor (ºC)	935	935	935	935	935	935
	Fe_2O_3 flow in the Fuel Reactor (kg/h)	3500	3500	3500	3500	3500	3500
	Al_2O_3 in the System (kg/h)	1500	1500	1500	1500	1500	1500
	Particle Density (kg/m³)	3200	3200	3200	3200	3200	3200
Energy balance (kW)	Fuel Reactor	221.47	221.47	221.47	221.47	221.47	221.47
	Air Reactor	475.99	476.14	476.28	476.42	476.56	476.99
	Cool air reactor exhaust	168.10	192.35	216.60	240.88	265.09	337.84
	Cool flue gas	115.40	115.40	115.40	115.40	115.40	115.40
	Cool OC for air reactor	19.83	19.83	19.83	19.83	19.83	19.83
	Reheat OC for fuel reactor	-20.83	-20.83	-20.83	-20.83	-20.83	-20.83
	Heat steam	-69.80	-69.80	-69.80	-69.80	-69.80	-69.80
	Heat air	-206.59	-232.41	-258.23	-284.06	-309.88	-387.35
	Net	703.58	702.15	700.71	699.32	697.85	693.55

Table A.23 CLC process simulation results for different air flow rates with Lignite coal at 100 kg/h and Fe_2O_3/Al_2O_3 at 4000/2000 kg/h

Initial values	Coal (kg/h)	100	100	100	100	100	100
	Water (kg/h)	140	140	140	140	140	140
	Air Flow Rate (kg/h)	100	300	400	500	600	713
	Temperature of Fuel Reactor (ºC)	950	950	950	950	950	950
	Temperature of Air Reactor (ºC)	935	935	935	935	935	935
	Fe_2O_3 flow in the Fuel Reactor (kg/h)	4000	4000	4000	4000	4000	4000
	Al_2O_3 in the System (kg/h)	2000	2000	2000	2000	2000	2000
	Particle Density (kg/m³)	3200	3200	3200	3200	3200	3200
Energy balance (kW)	Fuel Reactor	226.51	226.51	226.51	226.51	226.51	226.51
	Air Reactor	96.50	289.50	386.00	475.59	475.72	475.87
	Cool air reactor exhaust	19.00	56.99	75.99	95.36	119.61	147.01
	Cool flue gas	115.40	115.40	115.40	115.40	115.40	115.40
	Cool OC for air reactor	24.31	24.31	24.31	24.31	24.31	24.31
	Reheat OC for fuel reactor	-25.31	-25.31	-25.31	-25.31	-25.31	-25.31
	Heat steam	-69.80	-69.80	-69.80	-69.80	-69.80	-69.80
	Heat air	-25.82	-77.47	-103.29	-129.12	-154.94	-184.10
	Net	360.77	540.11	629.79	712.93	711.48	709.88
Initial values	Coal (kg/h)	100	100	100	100	100	100
	Water (kg/h)	140	140	140	140	140	140
	Air Flow Rate (kg/h)	800	900	1000	1100	1200	1500
	Temperature of Fuel Reactor (ºC)	950	950	950	950	950	950
	Temperature of Air Reactor (ºC)	935	935	935	935	935	935
	Fe_2O_3 flow in the Fuel Reactor (kg/h)	4000	4000	4000	4000	4000	4000
	Al_2O_3 in the System (kg/h)	2000	2000	2000	2000	2000	2000
	Particle Density (kg/m³)	3200	3200	3200	3200	3200	3200
Energy balance (kW)	Fuel Reactor	226.51	226.51	226.51	226.51	226.51	226.51
	Air Reactor	475.99	476.14	476.28	476.42	476.56	476.99
	Cool air reactor exhaust	168.10	192.35	216.60	240.88	265.09	337.84
	Cool flue gas	115.40	115.40	115.40	115.40	115.40	115.40
	Cool OC for air reactor	24.31	24.31	24.31	24.31	24.31	24.31
	Reheat OC for fuel reactor	-25.31	-25.31	-25.31	-25.31	-25.31	-25.31
	Heat steam	-69.80	-69.80	-69.80	-69.80	-69.80	-69.80
	Heat air	-206.59	-232.41	-258.23	-284.06	-309.88	-387.35
	Net	708.61	707.17	705.74	704.35	702.87	698.58

Table A.24 CLC process simulation results for different air flow rates with Lignite coal at 100 kg/h and Fe_2O_3/Al_2O_3 at 4500/2500 kg/h

Initial values	Coal (kg/h)	100	100	100	100	100	100
	Water (kg/h)	140	140	140	140	140	140
	Air Flow Rate (kg/h)	100	300	400	500	600	713
	Temperature of Fuel Reactor (ºC)	950	950	950	950	950	950
	Temperature of Air Reactor (ºC)	935	935	935	935	935	935
	Fe_2O_3 flow in the Fuel Reactor (kg/h)	4500	4500	4500	4500	4500	4500
	Al_2O_3 in the System (kg/h)	2500	2500	2500	2500	2500	2500
	Particle Density (kg/m³)	3200	3200	3200	3200	3200	3200
Energy balance (kW)	Fuel Reactor	231.54	231.54	231.54	231.54	231.54	231.54
	Air Reactor	96.50	289.50	386.00	475.59	475.72	475.87
	Cool air reactor exhaust	19.00	56.99	75.99	95.36	119.61	147.01
	Cool flue gas	115.40	115.40	115.40	115.40	115.40	115.40
	Cool OC for air reactor	28.78	28.78	28.78	28.78	28.78	28.78
	Reheat OC for fuel reactor	-29.79	-29.79	-29.79	-29.79	-29.79	-29.79
	Heat steam	-69.80	-69.80	-69.80	-69.80	-69.80	-69.80
	Heat air	-25.82	-77.47	-103.29	-129.12	-154.94	-184.10
	Net	365.79	545.14	634.81	717.96	716.50	714.90
Initial values	Coal (kg/h)	100	100	100	100	100	100
	Water (kg/h)	140	140	140	140	140	140
	Air Flow Rate (kg/h)	800	900	1000	1100	1200	1500
	Temperature of Fuel Reactor (ºC)	950	950	950	950	950	950
	Temperature of Air Reactor (ºC)	935	935	935	935	935	935
	Fe_2O_3 flow in the Fuel Reactor (kg/h)	4500	4500	4500	4500	4500	4500
	Al_2O_3 in the System (kg/h)	2500	2500	2500	2500	2500	2500
	Particle Density (kg/m³)	3200	3200	3200	3200	3200	3200
Energy balance (kW)	Fuel Reactor	231.54	231.54	231.54	231.54	231.54	231.54
	Air Reactor	475.99	476.14	476.28	476.42	476.56	476.99
	Cool air reactor exhaust	168.10	192.35	216.60	240.88	265.09	337.84
	Cool flue gas	115.40	115.40	115.40	115.40	115.40	115.40
	Cool OC for air reactor	28.78	28.78	28.78	28.78	28.78	28.78
	Reheat OC for fuel reactor	-29.79	-29.79	-29.79	-29.79	-29.79	-29.79
	Heat steam	-69.80	-69.80	-69.80	-69.80	-69.80	-69.80
	Heat air	-206.59	-232.41	-258.23	-284.06	-309.88	-387.35
	Net	713.63	712.20	710.76	709.37	707.90	703.60

Appendix B Simulation Results of CLOU

Table B.1 CLOU process simulation results for different air flow rates with Bituminous coal at 256 g/h and CuO at 9 kg/h

Amount of OC (kg/h)	9	9	9	9	9	9	9	9	9
Air flow rate (l/h)	800	1000	1500	1800	1980	2200	2500	3000	3500
Q-A (W)	165.23	193.44	257.26	209.18	180.30	145.08	97.00	16.87	-63.26
Q-Burn (W)	1776.88	1776.88	1776.88	1776.88	1776.88	1776.88	1776.88	1776.88	1776.88
Q-C-A (W)	129.51	161.89	243.61	302.73	338.20	381.55	440.67	539.19	637.72
Q-C-F (W)	269.30	269.30	269.30	269.30	269.30	269.30	269.30	269.30	269.30
Q-Decomp (W)	120.65	120.65	120.65	120.65	120.65	120.65	120.65	120.65	120.65
Q-F (W)	-1094.00	-1094.00	-1094.00	-1094.00	-1094.00	-1094.00	-1094.00	-1094.00	-1094.00
Total power (W)	1367.57	1428.16	1573.71	1584.74	1591.33	1599.46	1610.50	1628.90	1647.30

Table B.2 CLOU process simulation results for different air flow rates with Anthracite coal at 256 g/h and CuO at 9 kg/h

Amount of OC (kg/h)	9	9	9	9	9	9	9	9	9
Air flow rate (l/h)	800	1000	1500	1800	1980	2200	2500	3000	3500
Q-A (W)	165.23	193.44	257.26	209.18	180.30	145.08	97.00	16.87	-63.26
Q-Burn (W)	1621.58	1621.58	1621.58	1621.58	1621.58	1621.58	1621.58	1621.58	1621.58
Q-C-A (W)	129.51	161.89	243.61	302.73	338.20	381.55	440.67	539.19	637.72
Q-C-F (W)	247.38	247.38	247.38	247.38	247.38	247.38	247.38	247.38	247.38
Q-Decomp (W)	343.56	343.56	343.56	343.56	343.56	343.56	343.56	343.56	343.56
Q-F (W)	-1094.00	-1094.00	-1094.00	-1094.00	-1094.00	-1094.00	-1094.00	-1094.00	-1094.00
Total power (W)	1413.26	1473.85	1619.39	1630.43	1637.02	1645.15	1656.19	1674.58	1692.98

Table B.3 CLOU process simulation results for different air flow rates with Lignite coal at 256 g/h and CuO at 9 kg/h

Amount of OC (kg/h)	9	9	9	9	9	9	9	9	9
Air flow rate (l/h)	800	1000	1500	1800	1980	2200	2500	3000	3500
Q-A (W)	165.23	193.44	257.26	209.18	180.30	145.08	97.00	16.87	-63.26
Q-Burn (W)	1189.46	1189.46	1189.46	1189.46	1189.46	1189.46	1189.46	1189.46	1189.46
Q-C-A (W)	129.51	161.89	243.61	302.73	338.20	381.55	440.67	539.19	637.72
Q-C-F (W)	250.37	250.37	250.37	250.37	250.37	250.37	250.37	250.37	250.37
Q-Decomp (W)	512.84	512.84	512.84	512.84	512.84	512.84	512.84	512.84	512.84
Q-F (W)	-1094.00	-1094.00	-1094.00	-1094.00	-1094.00	-1094.00	-1094.00	-1094.00	-1094.00
Total power (W)	1153.41	1214.00	1359.54	1370.58	1377.17	1385.30	1396.34	1414.73	1433.13

Table B.4 CLOU process simulation results for different air flow rates with Bituminous coal at 256 g/h and Co_3O_4 at 13.5 kg/h

Amount of OC (kg/h)	13.5	13.5	13.5	13.5	13.5	13.5	13.5	13.5
Air flow rate (l/h)	1000	1500	1800	1980	2200	2500	3000	4000
Q-A (W)	412.84	561.32	513.25	484.41	449.15	401.08	320.96	160.72
Q-Burn (W)	1776.88	1776.88	1776.88	1776.88	1776.88	1776.88	1776.88	1776.88
Q-C-A (W)	161.89	243.74	302.85	338.32	381.68	440.79	539.32	736.37
Q-C-F (W)	269.06	269.06	269.06	269.06	269.06	269.06	269.06	269.06
Q-Decomp (W)	120.65	120.65	120.65	120.65	120.65	120.65	120.65	120.65
Q-F (W)	-1715.90	-1715.90	-1715.90	-1715.90	-1715.90	-1715.90	-1715.90	-1715.90
Total power (W)	1025.42	1255.75	1266.79	1273.42	1281.52	1292.56	1310.97	1347.78

Table B.5 CLOU process simulation results for different air flow rates with Bituminous coal at 256 g/h and Co_3O_4 at 13.5 kg/h

Amount of OC (kg/h)	13.5	13.5	13.5	13.5	13.5	13.5	13.5	13.5
Air flow rate (l/h)	1000	1500	1800	1980	2200	2500	3000	4000
Q-A (W)	412.84	561.32	513.25	484.41	449.15	401.08	320.96	160.72
Q-Burn (W)	1621.58	1621.58	1621.58	1621.58	1621.58	1621.58	1621.58	1621.58
Q-C-A (W)	161.89	243.74	302.85	338.32	381.68	440.79	539.32	736.37
Q-C-F (W)	247.10	247.10	247.10	247.10	247.10	247.10	247.10	247.10
Q-Decomp (W)	343.56	343.56	343.56	343.56	343.56	343.56	343.56	343.56
Q-F (W)	-1715.90	-1715.90	-1715.90	-1715.90	-1715.90	-1715.90	-1715.90	-1715.90
Total power (W)	1071.06	1301.40	1312.44	1319.07	1327.16	1338.21	1356.61	1393.43

Table B.6 CLOU process simulation results for different air flow rates with Bituminous coal at 256 g/h and Co_3O_4 at 13.5 kg/h

Amount of OC (kg/h)	13.5	13.5	13.5	13.5	13.5	13.5	13.5	13.5
Air flow rate (l/h)	1000	1500	1800	1980	2200	2500	3000	4000
Q-A (W)	412.84	561.32	513.25	484.41	449.15	401.08	320.96	160.72
Q-Burn (W)	1189.46	1189.46	1189.46	1189.46	1189.46	1189.46	1189.46	1189.46
Q-C-A (W)	161.89	243.74	302.85	338.32	381.68	440.79	539.32	736.37
Q-C-F (W)	250.08	250.08	250.08	250.08	250.08	250.08	250.08	250.08
Q-Decomp (W)	512.88	512.88	512.88	512.88	512.88	512.88	512.88	512.88
Q-F (W)	-1715.90	-1715.90	-1715.90	-1715.90	-1715.90	-1715.90	-1715.90	-1715.90
Total power (W)	811.25	1041.59	1052.63	1059.26	1067.35	1078.40	1096.80	1133.62

Table B.7 CLOU process simulation results for different air flow rates with Bituminous coal at 256 g/h and Mn_2O_3 at 26 kg/h

Amount of OC (kg/h)	26	26	26	26	26	26	26	26
Air flow rate (l/h)	800	1000	1500	1800	1980	2200	2500	3000
Q-A (W)	265.67	303.26	320.10	291.25	256.00	207.93	127.81	-32.43
Q-Burn (W)	1776.88	1776.88	1776.88	1776.88	1776.88	1776.88	1776.88	1776.88
Q-C-A (W)	161.89	242.83	292.25	327.72	371.07	430.19	528.71	725.77
Q-C-F (W)	275.40	275.40	275.40	275.40	275.40	275.40	275.40	275.40
Q-Decomp (W)	120.65	120.65	120.65	120.65	120.65	120.65	120.65	120.65
Q-F (W)	-1057.51	-1057.51	-1057.51	-1057.51	-1057.51	-1057.51	-1057.51	-1057.51
Total power (W)	1542.99	1661.51	1727.77	1734.40	1742.49	1753.54	1771.94	1808.76

Table B.8 CLOU process simulation results for different air flow rates with Anthracite coal at 256 g/h and Mn_2O_3 at 26 kg/h

Amount of OC (kg/h)	26	26	26	26	26	26	26	26
Air flow rate (l/h)	800	1000	1500	1800	1980	2200	2500	3000
Q-A (W)	265.67	303.26	320.10	291.25	256.00	207.93	127.81	-32.43
Q-Burn (W)	1621.56	1621.56	1621.56	1621.56	1621.56	1621.56	1621.56	1621.56
Q-C-A (W)	161.89	242.83	292.25	327.72	371.07	430.19	528.71	725.77
Q-C-F (W)	253.44	253.44	253.44	253.44	253.44	253.44	253.44	253.44
Q-Decomp (W)	343.56	343.56	343.56	343.56	343.56	343.56	343.56	343.56
Q-F (W)	-1057.51	-1057.51	-1057.51	-1057.51	-1057.51	-1057.51	-1057.51	-1057.51
Total power (W)	1588.61	1707.14	1773.39	1780.02	1788.12	1799.16	1817.57	1854.38

Table B.9 CLOU process simulation results for different air flow rates with Lignite coal at 256 g/h and Mn_2O_3 at 26 kg/h

Amount of OC (kg/h)	9	9	9	9	9	9	9	9
Air flow rate (l/h)	800	1000	1500	1800	1980	2200	2500	3000
Q-A (W)	265.674	303.257	320.095	291.251	255.998	207.926	127.806	-32.4342
Q-Burn (W)	1189.45	1189.45	1189.45	1189.45	1189.45	1189.45	1189.45	1189.45
Q-C-A (W)	161.886	242.829	292.249	327.718	371.07	430.186	528.712	725.765
Q-C-F (W)	253.761	253.761	253.761	253.761	253.761	253.761	253.761	253.761
Q-Decomp (W)	512.844	512.844	512.844	512.844	512.844	512.844	512.844	512.844
Q-F (W)	-1057.51	-1057.51	-1057.51	-1057.51	-1057.51	-1057.51	-1057.51	-1057.51
Total power (W)	1326.105	1444.631	1510.889	1517.514	1525.613	1536.657	1555.063	1591.8758

References

[1] Sahir A.H., Cadore A.L., Dansie J.K. (2012) *Process analysis of chemical looping with oxygen uncoupling (CLOU) and chemical looping combustion (CLC) for solid fuels*, 2nd International Conference on Chemical looping, Darmstadt, Germany.

[2] Abad A., Adanez-Rubio I., Gayan P., Garcia-Labiano F., de Diego L., Adanez J. (2012)*Demonstration of chemical-looping with oxygen uncoupling (CLOU) process in a 1.5 kWth continuously operating unit using a Cu-based oxygen-carrier*, Int. J. Greenhouse Gas Control 6, pp. 189-200.

[3] Parker J. (2012) *Simulation of Coal Particles in a Full Chemical Looping Combustion System.* CPFD Software, LLC, Albuquerque.

[4] Cuadrat A., Abad A., de Diego L.F. (2012) P*rompt considerations on the design of chemical looping combustion of coal from experimental tests*, Fuel 97, pp. 219-232.

[5] Wang J., Anthony E.J. (2008) *Clean combustion of solid fuels*, Applied Energy 85 (2), pp. 73-79.

[6] Gnanapragasam N.V., Reddy B.V., Rosen M.A. (2009) *Hydrogen production from coal using coal direct chemical looping and syngas chemical looping combustion systems: assessment of system operation and resource requirements*, Int. J. Hydrogen Energy 34 (6), pp. 2606-2615.

[7] Adánez J., Gayán P., Celaya J. (2006) *Chemical looping combustion in a 10 kWth prototype using a CuO/Al_2O_3 oxygen carrier: Effect of operating conditions on methane combustion*, Industrial & Engineering Chemistry Research 45 (17), pp. 6075-6080.

[8] Arjmand M., Azad A.M., Leion H., Lyngfelt A., Mattisson T. (2011) *Prospects of Al_2O_3 and MgAl2O4-supported CuO oxygen carriers in chemical-looping combustion (CLC) and chemical looping with oxygen uncoupling (CLOU)*, Energy & Fuels 25 (11), pp. 5493-5502.

[9] Leion H., Lyngfelt A., Johansson M., Jerndal E., Mattisson T. (2008) *The use of ilmenite as an oxygen carrier in chemical-looping combustion*, Chemical Engineering Research and Design 86 (9), pp. 1017-1026.

[10] Leion H., Mattisson T., Lyngfelt A. (2009) *Using chemical-looping with oxygen uncoupling (CLOU) for combustion of six different solid fuels*, Energy Procedia 1 (1), pp. 447-453.

[11] Mattisson T., Lyngfelt A., Leion H. (2009) *Chemical-looping with oxygen uncoupling for combustion of solid fuels*, Int. J. Greenhouse Gas Control 3 (1), pp. 11-19.

[12] Cuadrat A., Abad A., Adánez J., de Diego L.F. (2012) *Behavior of ilmenite as oxygen carrier in chemical looping combustion*, Fuel Processing Technology 94 (1), pp. 101-112.

[13] Mukherjee S., Kumar P., Hosseini A. (2014) *Comparative assessment of gasification based coal power plants with various CO_2 capture technologies producing electricity and hydrogen*, Energy & Fuels 28 (2), pp. 1028-1040.

[14] Zhou L., Zhang Z., Chivetta C., Agarwal R. (2013) *Process simulation and validation of chemical-looping with oxygen uncoupling (CLOU) process using Cu-based oxygen carrier*, Energy & Fuels 27, pp. 6906-6912.

[15] Hossain M M, de Lasa H I. (2008) *Chemical-looping combustion (CLC) for inherent CO_2 separations—a review,* J. of Chemical Engineering Science, 63(18): 4433-4451.

[16] ANSYS (2012) *ANSYS FLUENT User's Guide*, Canonsburg, PA.

[17] ANSYS (2012) *ANSYS FLUENT Theory Guide*, Canonsburg, PA.

[18] Zhang, Z., Zhou, L., and Agarwal, R. (2013) *Transient Simulations of Spouted Fluidized Bed for Coal-Direct Chemical Looping Combustion,* Energy Fuels, 28(2), pp. 1548–1560

[19] Link, J. M. (1975) *Development and Validation of a Discrete Particle Model of a Spout-Fluid Bed Granulator*, Ph.D. dissertation, University of Twente, Enschede, The Netherlands.

[20] Peng Z, Doroodchi E, Alghamdi Y A, et al. (2015) *CFD–DEM simulation of solid circulation rate in the cold flow model of chemical looping systems,* J. of Chemical Engineering Research and Design, 95: 262-280.

[21] Patankar, N.A., Joseph, D.D. (2001) *Modeling and numerical simulation of particulate flows by the Eulerian–Lagrangian approach.* Int. J. Multiphase Flow 27, 1659–1684.

Vita

Xiao Zhang

Degrees

M.S. Mechanical Engineering,
Washington University in St. Louis, August 2015

B.E. Thermal and Power Engineering,
Chongqing University, June 2013

Publications

Zhang, Xiao, et al. "Process simulation and maximization of energy output in chemical-looping combustion using ASPEN plus." Journal homepage: www. IJEE. IEEFoundation. org 6.2 (2015): 201-226.

Zhang, Xiao, et al. "Validation of chemical-looping with oxygen uncoupling (CLOU) using Cu-based oxygen carrier and comparative study of Cu, Mn and Co based oxygen carriers using ASPEN plus." Journal homepage: www. IJEE. IEEFoundation. org 6.3 (2015): 247-254.

August 2015